Development of a Highly Specific 18F-labeled Radioligand for Imaging of Sigma-2 Receptor in Brain Tumor

Wang, T.; Wang, J.; Chen, L.; Zhang, X.; Mou, T.; An, X.; Zhang, J.; Zhang, X.; Deuther-Conrad, W.; Huang, Y.; Jia, H.;

Originally published:

September 2023

Journal of Medicinal Chemistry 66(2023)18, 12840-12857

DOI: https://doi.org/10.1021/acs.jmedchem.3c00735

Development of a Highly Specific ^{18}F-labeled Radioligand for Imaging of Sigma-2 Receptor in Brain Tumor

Tao Wang[a, b, #], Jingqi Wang[a, #], Leyuan Chen[c], Xiaojun Zhang[d], Tiantian Mou[e], Xiaodan An[a], Jinming Zhang[d,*], Xiaoli Zhang[e], Winnie Deuther-Conrad[f], Yiyun Huang[g,*], Hongmei Jia[a,*]

[a] Key Laboratory of Radiopharmaceuticals (Beijing Normal University), Ministry of Education, College of Chemistry, Beijing Normal University, Beijing 100875, China

[b] Department of Nuclear Medicine, Xinqiao Hospital, Army Medical University, Chongqing 400037, China

[c] Institute of Radiation Medicine, Peking Union Medical College & Chinese Academy of Medical Sciences, Tianjin 300192, China

[d] Department of Nuclear Medicine, The First Medical Center of Chinese PLA General Hospital, Beijing 100853, China

[e] Department of Nuclear Medicine, Beijing Anzhen Hospital, Capital Medical University, Beijing 100029, China

[f] Helmholtz-Zentrum Dresden-Rossendorf (HZDR), Institute of Radiopharmaceutical Cancer Research, Department of Neuroradiopharmaceuticals, 04318 Leipzig, Germany

[g] Yale PET Center, Department of Radiology and Biomedical Imaging, Yale University School of Medicine, New Haven, CT 06520-8048, United States

*Corresponding authors:

*Phone: +86-10-58807843; Fax: +86-10-58802750. E-mail: hmjia@bnu.edu.cn (H Jia)

*Phone: +1-203-7853193; Fax: +1-203-7852994. E-mail: henry.huang@yale.edu (Y Huang)

*Phone: +86-10-68282330; Fax: +86-10-68282330. E-mail: zhangjm301@163.com (J Zhang)

[#] Tao Wang and Jingqi Wang contributed equally to this work.

ABSTRACT

Novel ligands with the 6,7-dimethoxy-1,2,3,4-tetrahydroisoquinoline or 5,6-dimethoxyisoindoline pharmacophore were designed and synthesized for evaluation of their structure-activity relationship to the sigma-2 (σ_2) receptor and developed as suitable PET radioligands. Compound **1** was found to possess nanomolar affinity ($K_i(\sigma_1)$ = 2.57 nM) for the σ_2 receptor, high subtype selectivity (> 2,000-fold) and high selectivity over 40 other receptors and transporters. Radioligand [^{18}F]**1** was prepared with radiochemical yield of 37–54%, > 99% radiochemical purity, and molar activity of 107–189 GBq/μmol. Biodistribution and blocking studies in mice and micro-PET/CT imaging of [^{18}F]**1** in rats indicated excellent binding specificity to the σ_2 receptors *in vivo*. Micro-PET/CT imaging of [^{18}F]**1** in the U87MG glioma xenograft model demonstrated clear tumor visualization with high tumor uptake and tumor-to-background ratio. Co-injection with CM398 (5 μmol/kg) led to remarkable reduction of tumor uptake (80%, 60–70 min), indicating high specific binding of [^{18}F]**1** in U87MG glioma xenografts.

Keywords: σ_2 receptor, benzimidazolone derivatives, brain tumor, positron emission tomography, fluorine-18

INTRODUCTION

The sigma-2 (σ_2) receptor is one subtype of the sigma (σ) receptors[1], and has been identified as transmembrane protein 97 (TMEM97)[2], which is also named meningioma-associated protein (MAC30) and plays a critical role in cholesterol homeostasis regulation[3]. Different from the sigma-1 (σ_1) receptor, the bovine σ_2 receptor/TMEM97 is a four-helix transmembrane bundle based on the high-resolution crystal structures of the σ_2 receptor in complex with roluperidone (MIN-101) and PB28[4]. The σ_2 receptor/TMEM97 has attracted increasing interests due to its involvements in the pathophysiology of various cancers[5-7], and brain disorders including Alzheimer's disease (AD), Parkinson's disease (PD), schizophrenia, neuropathic pain, drug addiction and depression[5, 8-15] CT1812, an antagonist of the σ_2 receptor, has proved to be effective for the treatment of AD in clinical trials[8, 9, 15]. In the past decades, the σ_2 receptor/TMEM97 has been proposed as a biomarker for the proliferative status of solid tumors in light of its approximately 10-fold higher expression in proliferating than quiescent tumors[6, 7, 16-20]. The σ_2 receptor/TMEM97, progesterone receptor membrane component 1 (PGRMC1) and low-density lipoprotein receptor (LDLR) were reported to form a trimeric complex to accelerate the internalization of LDL in proliferating versus quiescent tumor cells[21]. In addition, the σ_2 receptors/TMEM97 has also been regarded as a potential therapeutic target in human glioma[22], squamous cell carcinoma of lung (SQCLC)[23], gastric cancer[24], colorectal cancer (CRC)[25], nasopharyngeal carcinoma[26], hepatocellular carcinoma (HCC)[27], breast cancer[28] and pancreatic cancer[29]. Therefore, non-invasive positron emission tomography (PET) imaging with suitable radioligand of high affinity, selectivity and specificity for the σ_2 receptor/TMEM97 can visualize the proliferative status of tumors and help monitor the mechanism and treatment effects of new therapeutic approaches.

Over the years a number of radioligands targeting the σ_2 receptors have been developed for tumor imaging[6, 7, 30, 31]. One radiotracer, *N*-(4-(6,7-dimethoxy-3,4-dihydroisoquinolin-2(1*H*)-yl)butyl)-2-(2-fluoroethyl)-5-methylbenzamide ([^{18}F]ISO-1), has entered clinical trials for PET imaging of σ_2 receptors in tumors[19, 20]. However, its affinity for the σ_2 receptors ($K_i(\sigma_2)$ = 6.95–28.2 nM) and subtype selectivity ($K_i(\sigma_1)/K_i(\sigma_2)$ = 4–48) are relatively low and thus could be improved further[32-34]. In our

previous work, we developed a series of σ_2 receptor ligands with the 6,7-dimethoxy-1,2,3,4-tetrahydroisoquinoline or 5,6-dimethoxyisoindoline pharmacophore[32, 35-37]. Among these ligands, [^{18}F]SYB4 was found to display excellent biological profiles including nanomolar affinity, high subtype selectivity, high brain uptake, good specific binding and appropriate kinetics in the brain[36-38]. Recently, 1-(4-(6,7-dimethoxy-3,4-dihydroisoquinolin-2(1*H*)-yl)butyl)-3-methyl-1*H*-benzo[*d*]imidazol-2(3*H*)-one (CM398) was reported as a σ_2 receptor ligand with high affinity ($K_i(\sigma_2)$ = 0.43 nM) and subtype selectivity ($K_i(\sigma_1)$ = 560 nM, $K_i(\sigma_1)/K_i(\sigma_2)$ = 1,302)[39, 40]. In the current work, we used SYB4 and CM398 as lead compounds to design and develop suitable ^{18}F-labeled radioligands for imaging the σ_2 receptor in brain tumors. The design concept is presented in Figure 1. First, we replaced the methyl group with fluoroethyl (**1**) or introduced a fluoroethoxy group at the benzimidazolone ring (**2**) of CM398 to enable the incorporation of ^{18}F for PET imaging. Second, we incorporate the benzimidazole ring instead of the indole ring of SYB4 with the 5,6-dimethoxyisoindoline or 6,7-dimethoxy-1,2,3,4-tetrahydroisoquinoline scaffold to decrease the lipophilicity (**3**–**6**). Third, to further simplify the structure and investigate the structure-activity relationship, we replaced the benzimidazolone ring with the benzene ring and introduced various fluorine-containing substituents at the *para*- or *meta*-position (**7**–**14**). Herein we report the synthesis and *in vitro* assays of these novel compounds, as well as the preparation and *in vivo* evaluation of a new ^{18}F-labeled radioligand for its potential to image the σ_2 receptors in glioma.

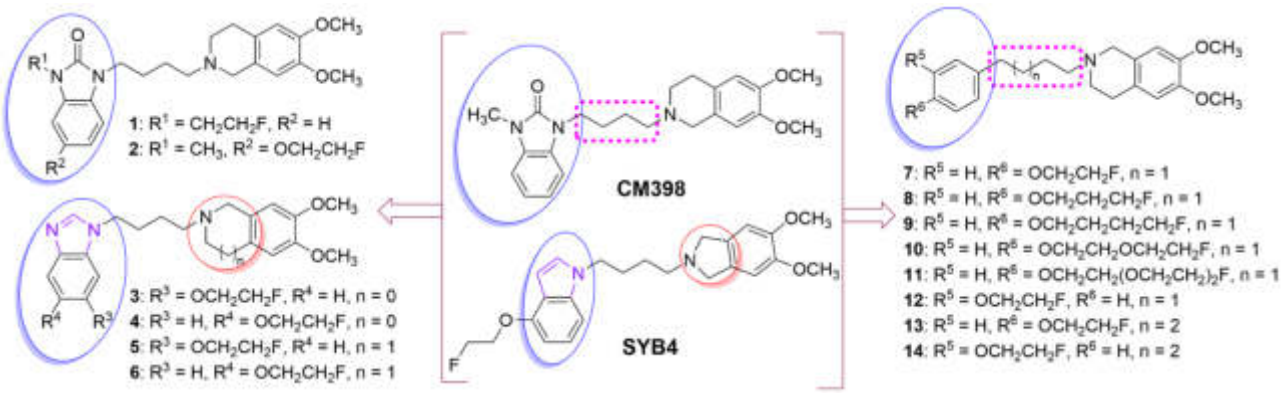

Figure 1. Design concept of benzimidazolone-, benzimidazole- and benzene-based derivatives as new σ_2 receptor ligands.

RESULTS

Chemistry. Compound 6,7-dimethoxy-1,2,3,4-tetrahydroisoquinoline is commercially available. The 5,6-dimethoxyisoindoline (**S4**) and substrates **S5**–**S9** were prepared following the methods reported previously[35, 41] with minor modifications, as shown in Supporting Information Scheme S1 and S2. Benzimidazolone-based compounds **1**–**2** are derivatives of CM398[39, 40]. Compound **1**, derived from CM398 by replacement of the methyl with a fluoroethyl moiety, was prepared *via* a five-step route as shown in Scheme 1. Protection of compound **15** by *tert*-butyl carbonate provided intermediate **16**, followed by a nucleophilic substitution reaction with 1,4-dibromobutane to obtain compound **17**. *N*-Alkylation of the pharmacophore 6,7-dimethoxy-1,2,3,4-tetrahydroisoquinoline with compound **17** gave compound **18**, followed by hydrolysis of the *tert*-butyl carbonate group under acidic conditions to obtain compound **19**. Further reaction with 1-bromo-2-fluoroethane led to the target compound **1**.

Scheme 1. Synthetic route for benzimidazolone-based derivative **1**[a]

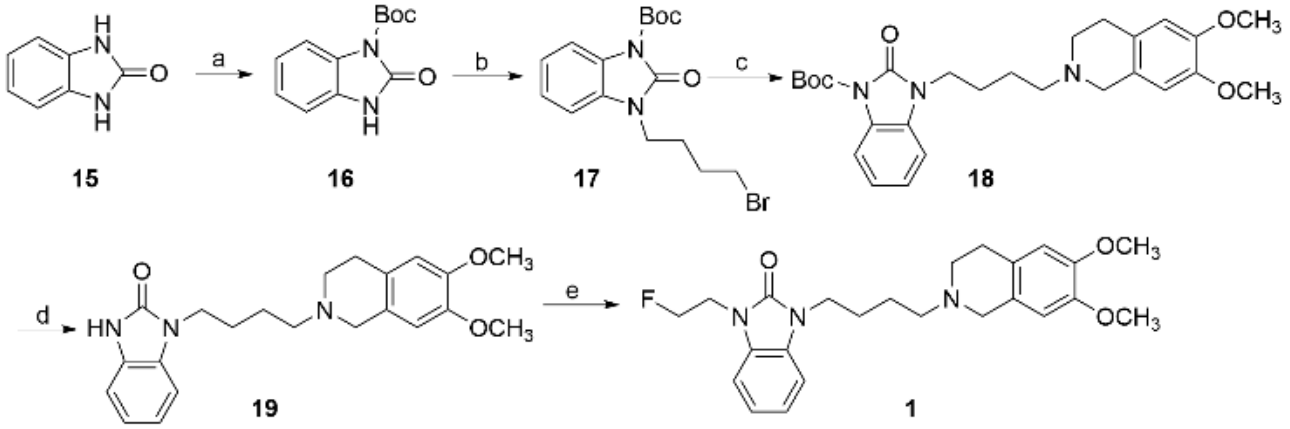

[a]Reagents and conditions: (a) $(Boc)_2O$, NaH, DMF, r.t., overnight, 92%; (b) 1,4-dibromobutane, K_2CO_3, TEA, DMF, 60 °C, overnight, 56%; (c) 6,7-dimethoxy-1,2,3,4-tetrahydroisoquinoline, K_2CO_3, TEA, MeCN, reflux, overnight, 53%; (d) TFA, CH_2Cl_2, r.t., overnight, 93%; (e) 1-bromo-2-fluoroethane, K_2CO_3, TBAI, DMF, 65 °C, overnight, 58%.

Scheme 2. Synthetic route for benzimidazolone-based derivative **2**[a]

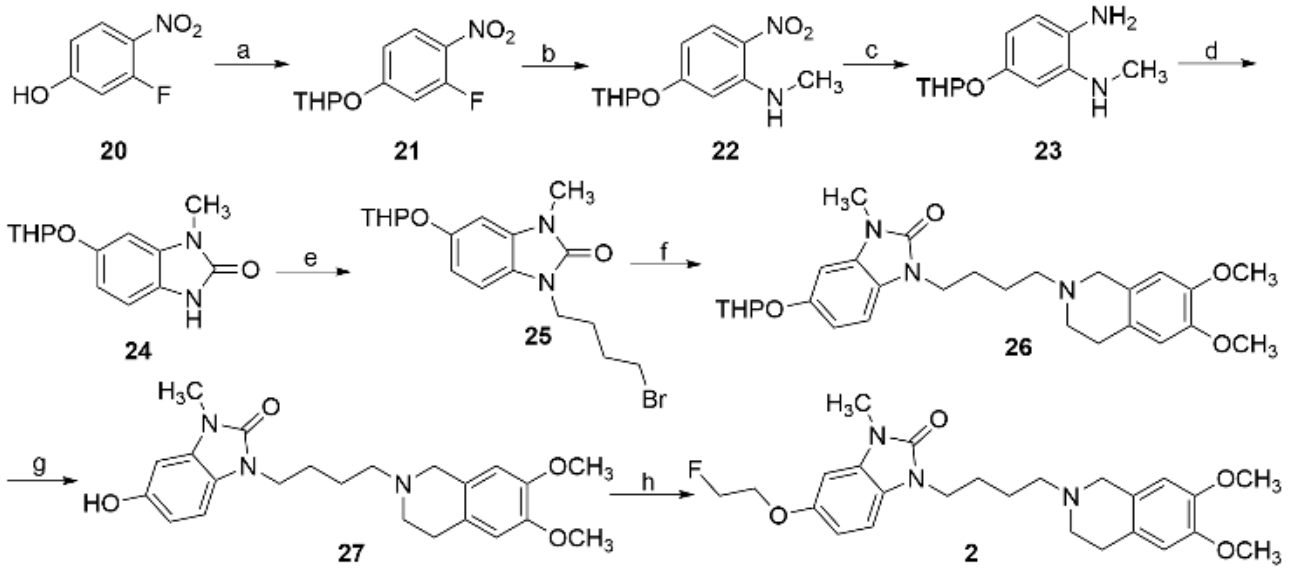

[a]Reagents and conditions: (a) DHP, TFA, CH_2Cl_2, r.t., 2 h, 98%; (b) $MeNH_2$, H_2O, r.t., overnight, 81%; (c) Pd/C, H_2, MeOH, 50 °C, overnight, 83%; (d) CDI, N_2, THF, 65 °C, overnight, 32%; (e) 1,4-dibromobutane, K_2CO_3, TBAI, DMF, 65 °C, 2 h, 58%; (f) 6,7-dimethoxy-1,2,3,4-tetrahydroisoquinoline, K_2CO_3, TEA, MeCN, reflux, overnight; (g) HCl (1 M in MeOH), MeOH, r.t., 1 h, 98%; (h) 1-bromo-2-fluoroethane, K_2CO_3, TEA, MeCN, reflux, overnight, 51%.

Compound **2** was synthesized *via* an eight-step route as presented in Scheme 2. Protection of the phenolic hydroxyl group in compound **20** with 3,4-dihydro-2*H*-pyran gave intermediate **21**, followed by amination of the fluorine substituent on the benzene ring and reduction of the nitro group to provide compounds **22** and **23**, respectively. Compound **23** was reacted with 1,1′-carbonyldiimidazole (CDI) to form urea **24**, followed by successive *N*-alkylation to obtain intermediates **25** and **26**, respectively. Cleavage of the THP protecting group followed by reaction of the phenol **27** with 1-bromo-2-fluoroethane then led to the target compound **2**.

Synthesis of benzimidazole-based derivatives **3**–**6** is shown in Scheme 3. Demethylation of 5- or 6-methoxybenzoimidazole (**28, 29**) followed by re-protection of the phenolic hydroxy group in **30** and **31** with *tert*-butyldimethylsilyl (TBS) gave compounds **32** and **33**. Compounds **36**–**39** were obtained by placement of the butyl linker between the secondary amine of imidazole in **32** and **33** and 6,7-

dimethoxy-1,2,3,4-tetrahydroisoquinoline or 5,6-dimethoxyisoindoline, followed by removal of the TBS protecting group. Alkylation of compounds **36**–**39** led to the target compounds **3**–**6**.

Scheme 3. Synthetic routes for benzimidazole-based derivatives **3**–**6**[a]

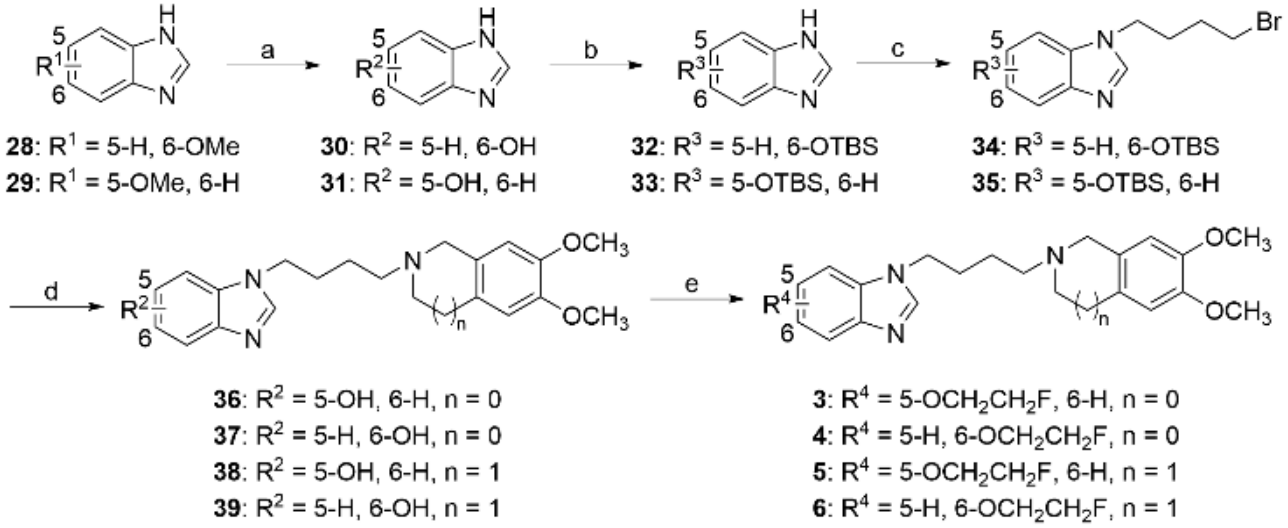

28: R^1 = 5-H, 6-OMe
29: R^1 = 5-OMe, 6-H

30: R^2 = 5-H, 6-OH
31: R^2 = 5-OH, 6-H

32: R^3 = 5-H, 6-OTBS
33: R^3 = 5-OTBS, 6-H

34: R^3 = 5-H, 6-OTBS
35: R^3 = 5-OTBS, 6-H

36: R^2 = 5-OH, 6-H, n = 0
37: R^2 = 5-H, 6-OH, n = 0
38: R^2 = 5-OH, 6-H, n = 1
39: R^2 = 5-H, 6-OH, n = 1

3: R^4 = 5-OCH_2CH_2F, 6-H, n = 0
4: R^4 = 5-H, 6-OCH_2CH_2F, n = 0
5: R^4 = 5-OCH_2CH_2F, 6-H, n = 1
6: R^4 = 5-H, 6-OCH_2CH_2F, n = 1

[a]Reagents and conditions: (a) HBr (48% in water), reflux, 6 h, 51%; (b) TBSCl, imidazole, CH_2Cl_2, 0 °C to r.t., 2 h, 85–87%; (c) 1,4-dibromobutane, Cs_2CO_3, NaI, DMF, 65 °C, 2 h, ; (d) 1) 6,7-dimethoxy-1,2,3,4-tetrahydroisoquinoline or 5,6-dimethoxyisoindoline (**S4**), K_2CO_3, TEA, MeCN, reflux, overnight; 2) TBAF (1 M in THF), THF, r.t., 1 h; (e) 2-fluoroethyl 4-methylbenzenesulfonate, KOH, TEA, MeCN, 90 °C, 1 h, 32–42%.

The benzene-based compounds **7**–**14** were synthesized *via* a six-step route, as shown in Scheme 4. Protection of the phenolic hydroxy group on substrates **40** and **41** with benzyl bromide (BnBr) led to compounds **42** and **43**, which underwent CuI-catalyzed Songashira cross-coupling with substrates **44** and **45** to give compounds **46**–**49**. Further Appel-Lee reaction with *tetra*-bromomethane (CBr_4) provided compounds **50**–**53**, which were then reacted with 6,7-dimethoxy-1,2,3,4-tetrahydroisoquinoline to afford compounds **54**–**57**, respectively. Pd/C-catalyzed hydrogenation of the alkyne and simultaneous removal of the Bn protecting group gave compounds **58**–**61**. Final alkylation with **S5**–**S9** then led to the target compounds **7**–**14**.

Scheme 4. Synthetic routes for benzene-based derivatives **7**–**14**[a]

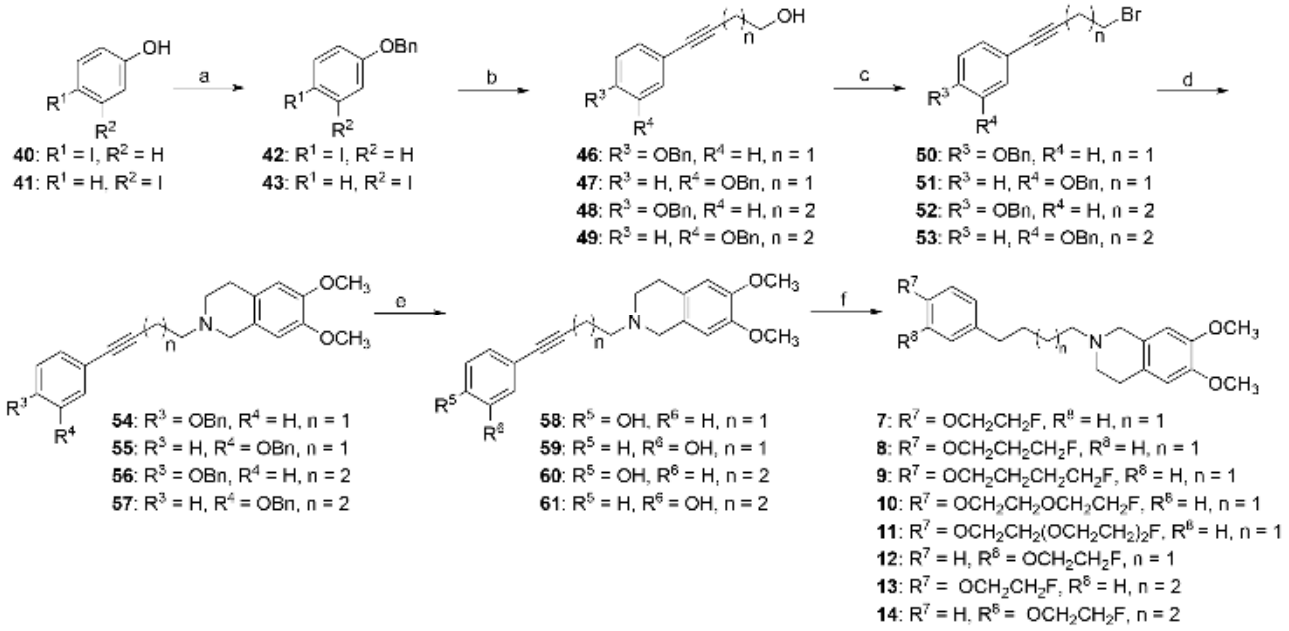

[a]Reagents and conditions: (a) BnBr, K_2CO_3, DMF, r.t., 2 h, 98%; (b) 3-butyn-1-ol (**44**) or 4-pentyn-1-ol (**45**), $(PPh_3)_2PdCl_2$, CuI, TEA, CH_2Cl_2, r.t. to 50 °C, overnight, 87–97%; (c) CBr_4, TPP, CH_2Cl_2, 0 °C to r.t., 12 h, 82–95%; (d) 6,7-dimethoxy-1,2,3,4-tetrahydroisoquinoline, K_2CO_3, NaI, MeCN, reflux, overnight, 42–60%; (e) Pd/C, H_2, MeOH, 50 °C, overnight, 75–89%; (f) **S5**–**S9**, KOH, TEA, MeCN, 90 °C, 0.5–1 h, 61–96%.

***In Vitro* Radioligand Competition Binding Studies.** Affinity of the novel ligands towards σ receptors were determined with radioligand competition binding assays by the National Institute of Mental Health (NIMH) Psychoactive Drug Screening Program (PDSP, https://pdsp.unc.edu/pdspweb/?site=assays) and the Helmholtz-Zentrum Dresden-Rossendorf (HZDR). The results are shown in Table 1. Replacement of the methyl group with fluoroethyl at the nitrogen atom or introduction of fluoroethoxy substituent on the benzene ring of the benzimidazolone scaffold only slightly decreased the affinity for the σ_2 receptors and subtype selectivity (**1**–**2** *vs.* CM398). Compounds **1**–**2** still maintained nanomolar affinity with $K_i(\sigma_2)$ values of 1.56–3.56 nM and high subtype selectivity towards the σ_1 receptor ($K_i(\sigma_1)/K_i(\sigma_2)$ > 2,000). However, replacement of the indole ring with the benzimidazole scaffold significantly decreased the σ_2 affinity (**3**–**6** *vs.* SYB4).

Benzimidazole-based derivatives **3**–**6** only displayed moderate affinity for the σ_2 receptor. It is interesting that replacement of the benzimidazolone with the benzene ring still preserved low nanomolar affinity for the σ_2 receptors with $K_i(\sigma_2)$ values of 2.78–7.23 nM (except for compound **11**). Compounds with the fluoroethoxy group at the different positions of the benzene ring also possessed high affinity for the σ_1 receptor and thus led to low subtype selectivity (compounds **7** and **12**–**14**). On the other hand, substitution at the *para*-position of the benzene ring with fluoropropoxy, fluorobutoxy or increased length of the fluorooligoethoxylated chain (n = 2, 3) decreased the affinity for the σ_1 receptor and thus increased the subtype selectivity (compounds **8**–**11**).

In addition, compound **1** exhibited high selectivity over 40 other receptors and transporters. Since compound **1** possessed low nanomolar affinity for the σ_2 receptor, high subtype selectivity and high selectivity over other receptors and transporters, and suitable lipophilicity, its corresponding radioligand [^{18}F]**1** was prepared and evaluated as a potential σ_2 receptor probe for tumor imaging. To investigate the *in vivo* properties of the benzimidazole derivatives, the corresponding ^{18}F-labeled form of compound **4**, with moderate σ_2 receptor affinity, was also synthesized and evaluated.

Table 1 Binding affinities of novel σ_2 receptor ligands[a]

Compd.	log*P* [b]	$K_i(\sigma_1)$ (nM)	$K_i(\sigma_2)$ (nM)	$K_i(\sigma_1)/K_i(\sigma_2)$
1	3.16	6.86×10^3, 5.67×10^3	1.58, 3.56	> 2,000
2	3.03	5.04×10^3, 4.73×10^3	1.56, 2.86	> 2,000
3	2.85	8.50×10^3, 3.51×10^4	21.0, 24.5	958
4	2.85	3.97×10^4, 2.63×10^4	15.3, 15.0	> 2,000
5	3.13	6.31×10^4, 3.18×10^4	12.7, 22.2	> 2,000
6	3.13	3.16×10^4, 3.23×10^4	53.1, 52.6	605
7	4.61	15.1, 23.4	4.86, 5.36	4
8	4.72	168, 142	4.45, 5.52	31
9	5.17	150, 275	5.26, 4.71	43

10	4.46	202, 209	5.60, 5.57	37
11	4.30	882, 1.89×10^3	16.4, 20.7	75
12	4.61	17.0, 40.6	2.78, 3.72	9
13	5.03	22.2, 27.3	4.16, 6.43	5
14	5.03	14.3, 23.6	7.23, 4.86	3
CM398[39]	2.97	560	0.43	1,302
SYB4[36]	3.61	371	1.79	207
ISO-1[32]	3.06	102	28.2	4
ISO-1[33]	3.06	330	6.95	48
ISO-1[34]	3.06	95.1	13.3	7

[a]Values are from two experiments (n = 2) performed in triplicate. Data for compounds **1**–**6** were obtained from HZDR. Data for compounds **7**–**14** were from the PDSP of NIMH.

[b]Calculated with ChemBioDraw.

Molecular Docking Studies. Crystal structure studies of the σ_2 receptor have indicated that amino acid residues Asp29, Asp56, Glu73 and Gln77 are crucial for the binding to ligands, which is mainly through non-covalent bonding such as hydrogen bonds, electrostatic and hydrophobic interactions, and salt bridges[2, 4, 42]. Molecular docking studies were conducted to investigate the possible interaction mode of ligands CM398, **1**–**4**, **7** and **12** with the σ_2 receptor. The method was referenced and revised from previous σ_2 receptor crystal (PDB code: 7MFI) recognition[4] by Schrödinger software. Ligands CM398, **1**–**4**, **7** and **12** could enter the active region of the σ_2 receptor protein crystal in a U-shaped conformation (Figures 2, S1 and S2).

Compound CM398 showed electrostatic (negative) interactions with amino acid residues Asp29 and Glu73. Additionally, Tyr150 formed π-cation with the nitrogen atom at the isoquinoline scaffold, and hydrogen bond with the oxygen atom of the carbonyl group on the benzimidazolone scaffold (2.1 Å), respectively. Hydrogen bonding of compound CM398 with the σ_2 receptor protein crystal occurred between the nitrogen atom on the isoquinoline scaffold with Asp29 (2.3 Å) and the oxygen

atom at the methoxy substituent of the isoquinoline benzene ring with Thr110 (3.5 Å), respectively. Asp29 formed salt bridge with the nitrogen atom on the isoquinoline scaffold.

Compared to CM398, the electrostatic (negative) interactions with amino acid residues Asp29, Asp56 (compound **2**, **3** and **12**) and Glu73 were observed between compounds **1**–**4**, **7** and **12** and the σ_2 receptor residues. Additionally, π-π stacking and π-cation were formed between the Tyr150 or Tyr50 and different functional groups of all compounds. The amino acid residues Asp29 (compounds **1**–**4** and **7**), Glu73 (compounds **3** and **4**) and Tyr150 (compound **12**) in the σ_2 receptor protein crystal formed a salt bridge interaction with the nitrogen atom on the isoquinoline or isoindoline scaffold.

Additionally, hydrogen bonding was observed between the σ_2 receptor residues and compounds **1**–**4** and **7**. Benzimidazolone-based compound **1** (CM398 derivative) showed hydrogen bond with the oxygen atom of the carbonyl group on the benzimidazolone scaffold (3.0 Å). Similar to compound **1**, hydrogen bonding (Tyr150 and Asp29, 3.2 Å and 2.5 Å) was observed between compound **2** and the σ_2 receptor residues. Hydrogen bonding of benzimidazole-based compound **3** with the σ_2 receptor protein crystal occurred between the oxygen atom at the fluoroacetoxyalkyl chain of benzimidazole benzene ring with Tyr150 (2.0 Å) and the oxygen atom at the methoxy substituent of the isoindoline benzene ring with Gln77 (3.3 Å), respectively. For compound **4**, Asp29 and Gln77 formed hydrogen bonds with the nitrogen atom on the isoindoline scaffold (2.0 Å) and the oxygen atom at the methoxy substituent on the isoindoline scaffold (2.5 Å), respectively. The benzene-based derivative **7** showed hydrogen bonding between Glu77 and the oxygen atom of methoxyl group (2.3 Å). Compared to compound **7**, there was no hydrogen bonding observed between compound **12** and the σ_2 receptor residues but other different combinations, such as negative electrostatic interaction (Asp56) and salt bridge (Tyr150). The results are depicted in Figures 2, S1 and S2. The receptor-ligand docking scores of compounds CM398, **1**–**4**, **7** and **12** with the σ_2 receptor crystal were -7.53, -7.73, -7.06, -5.79, -6.03, -6.68 and -6.73 kcal/mol, respectively.

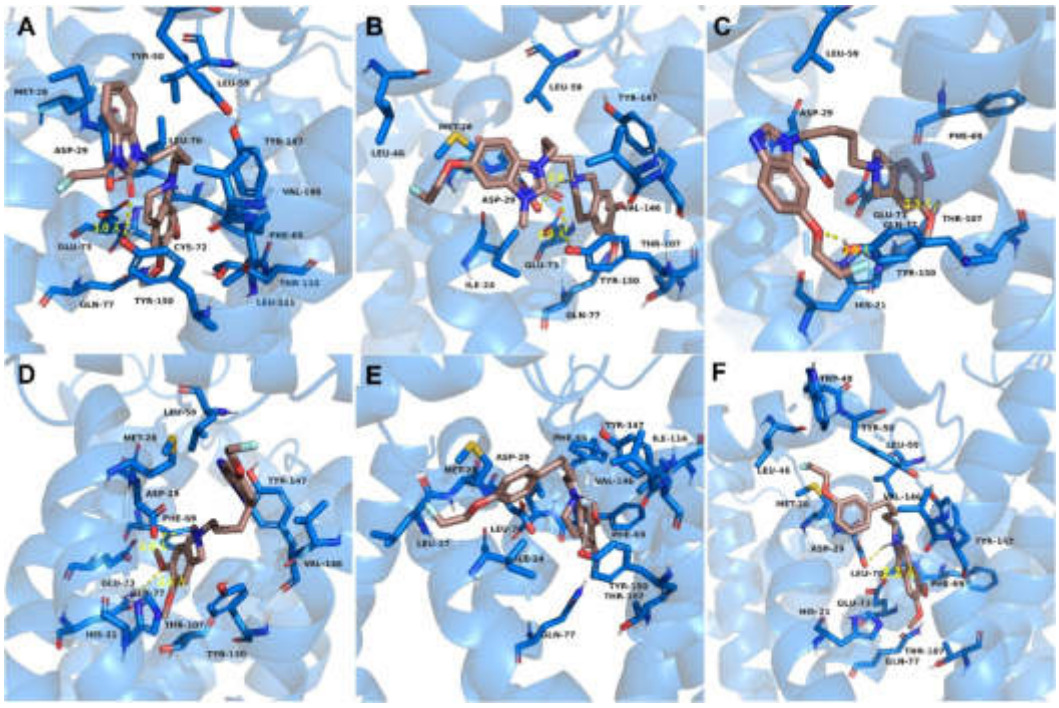

Figure 2. The docking of compounds **1** (A), **2** (B), **3** (C), **4** (D), **7** (E) and **12** (F) into the σ_2 receptor crystal, showing the poses of co-crystallized compounds and top-ranked docking (Carbon: sienna; Nitrogen: blue; Oxygen: red; Fluorine: pale cyan). Hydrogen bonds and distances are indicated by yellow dashed lines. In all panels, the σ_2 receptor is shown in royal-blue. PDB ID of σ_2 receptor crystal structure used as starting point for molecular modeling: 7MFI.

Radiochemistry.

Synthesis of the radiolabeling precursors **64** and **65** and radioligands [^{18}F]**1** and [^{18}F]**4** is outlined in Scheme 5. It was difficult to obtain precursor **64** via nucleophilic displacement of compound **19** with 1,2-bis(4-methylbenzenesulfonyloxy)ethane. Instead, compound **19** was reacted with (2-bromoethoxy)methyl)benzene to form intermediate **62**, followed by Pd/C-catalyzed reduction under hydrogen atmosphere to provide the hydroxyl intermediate **63**. Condensation with *p*-touenesulfonyl choride (TsCl) afforded precursor **64**. Coupling of intermediate **36** with 1,2-bis(4-methylbenzenesulfonyloxy)ethane provided precursor **65**.

Radioligands [^{18}F]**1** and [^{18}F]**4** were prepared through nucleophilic substitution as described previously[37]. Direct S_N2 displacement of the tosylate group in **64** and **65** with [^{18}F]fluoride in the form of Kryptofix 2.2.2/K^+/[^{18}F]F^- complex gave radioligands [^{18}F]**1** and [^{18}F]**4**, respectively. After

semipreparative HPLC purification, radioligands [^{18}F]**1** and [^{18}F]**4** were obtained in decay-corrected radiochemical yields (RCYs) of 37–54% (n = 3) and 1–3% (n = 2), respectively, with radiochemical purity (RCP) of more than 99%. The molar activity of [^{18}F]**1** and [^{18}F]**4** was 107–189 and 47–61 GBq/μmol, respectively, at the end of synthesis. The HPLC profiles for the identification of radioligands [^{18}F]**1** and [^{18}F]**4** are presented in Figures S3 and S4.

Scheme 5. Synthesis of the precursors (**64** and **65**) and radioligands ([^{18}F]**1** and [^{18}F]**4**)[a]

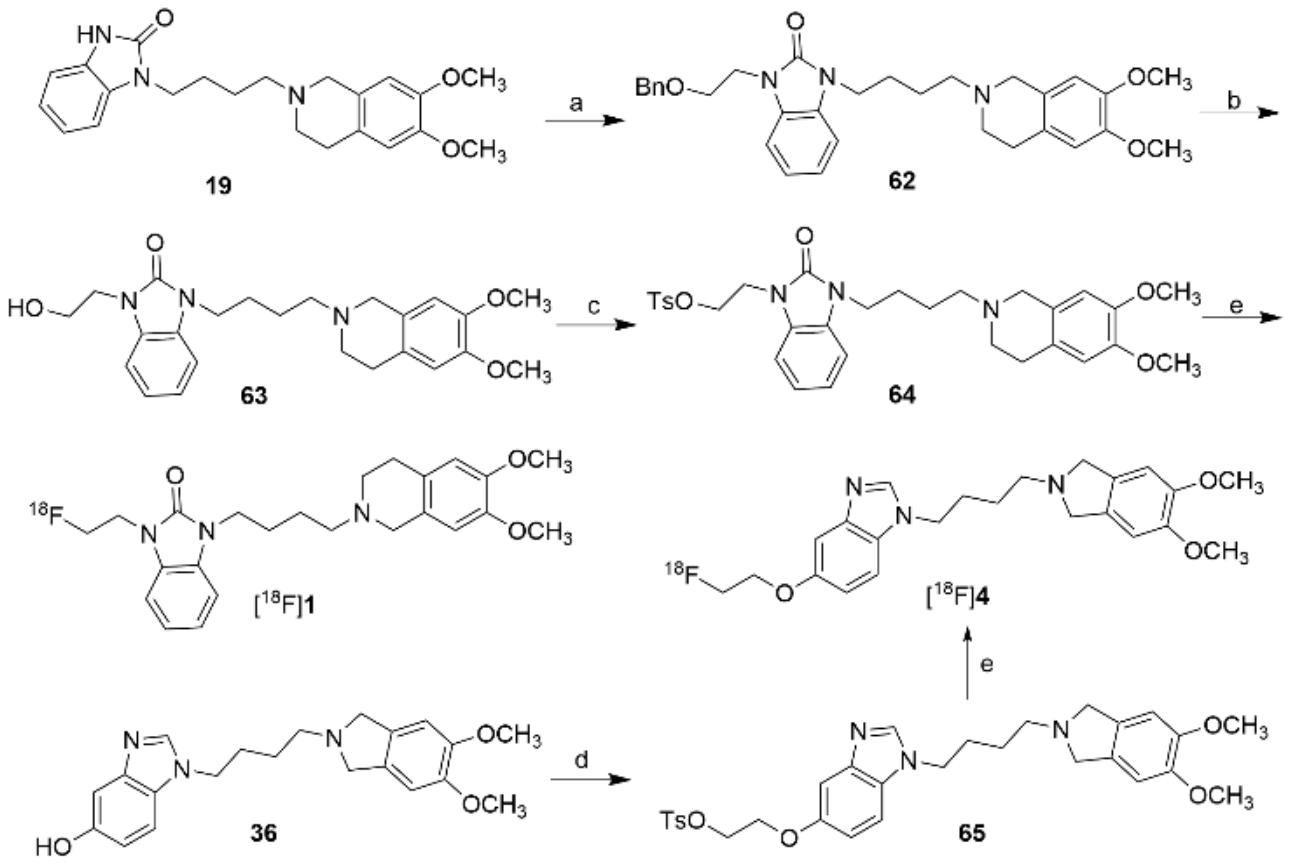

[a]Reagents and conditions: (a) ((2-bromoethoxy)methyl)benzene, K_2CO_3, TBAI, DMF, 60 °C, 2 h, 98%; (b) Pd/C, H_2, MeOH, 50 °C, overnight, 98%; (c) TsCl, TEA, DMAP, CH_2Cl_2, 0 °C to r.t., overnight, 78%. (d) 1,2-bis(4-methylbenzenesulfonyloxy)ethane, KOH, TEA, MeCN, 90 °C, 1 h, 53%; (e) $^{18}F^-$, Kryptofix 2.2.2, K_2CO_3, MeCN, 100 °C, 10 min.

Evaluation of Radioligands [^{18}F]1 and [^{18}F]4.

Lipophilicity. The apparent distribution coefficients of radioligands [^{18}F]**1** and [^{18}F]**4** were determined

using the shake-flask method as previously reported[37]. The log$D_{7.4}$ values were 1.78 ± 0.01 (n = 3) and 1.56 ± 0.02 (n = 3), respectively.

***In Vitro* Stability**. The *in vitro* stability of radioligands [^{18}F]**1** and [^{18}F]**4** in saline was evaluated by measuring the RCP at different time points using HPLC. After incubation with saline for 30, 60 and 120 min at room temperature, the RCP of [^{18}F]**1** was maintained at > 95%, while the RCP of [^{18}F]**4** was 95%, 87%, and 74%, respectively, as shown in Figure S5.

***Ex Vivo* Biodistribution and CM398 Blocking Studies in Mice.** Biodistribution studies of [^{18}F]**1** and [^{18}F]**4** were performed in male KM and ICR mice, respectively, to investigate their kinetic and *in vivo* binding properties. The results are presented in Tables 2 and S3, respectively. Radioligand [^{18}F]**1** exhibited moderate initial uptake in the brain (1.87 ± 0.31% ID/g at 2 min) and fast clearance, with 0.57 ± 0.07 and 0.18 ± 0.04% ID/g at 30 and 120 min, respectively. Radioactivity levels in the blood were very low with 0.53 ± 0.11 and 0.38 ± 0.08% ID/g at 30 and 60 min, respectively. Extremely high accumulation of radioactivity with about 50% ID/g at 120 min was observed in the pancreas, which has been shown to have high expression of the σ_2 receptors[43]. Radioactivity levels in the small intestines increased with time, indicating metabolism of the radiotracer through the hepatic-intestinal route and excretion into the small intestines. Finally, radioactivity uptake in the bone was very low (< 3% ID/g at 120 min), indicating no defluorination of radioligand [^{18}F]**1** *in vivo*.

Blocking studies with CM398 were carried out to investigate the specific binding of radioligands [^{18}F]**1** and [^{18}F]**4**. CM398 (5 μmol/kg of body weight) was injected 5 min prior to radioligand injection. As presented in Figure 3, Tables S2 and S4, pretreatment of animals with CM398 led to significant reduction in brain uptake levels (-37%, p = 0.001) and brain-to-blood ratios (-70%, p = 0.002). Moreover, remarkable reduction of radiotracer accumulation was also observed in the organs including heart (-33%, p = 0.005), kidney (-42%, p = 0.001), muscle (-44%, p = 0.002), liver (-50%, p < 0.001), spleen (-71%, p < 0.001), lung (-58%, p = 0.001), pancreas (-49%, p = 0.001) and bone (-70%, p = 0.003). These findings demonstrated highly specific binding of [^{18}F]**1** to the σ_2 receptors *in vivo*.

For radioligand [^{18}F]**4**, low accumulation in the brain (< 1% ID/g) was observed (Table S3). Moreover, blocking with CM398 led to significant reduction of radioactivity accumulation only in the pancreas (-80%, $p < 0.001$), as shown in Table S4. These results precluded further evaluation of [^{18}F]**4** *in vivo*.

Table 2. Biodistribution of [^{18}F]**1** in male KM mice[a]

Organ	2 min	15 min	30 min	60 min	120 min
Blood	1.54 ± 0.15	0.64 ± 0.10	0.53 ± 0.11	0.38 ± 0.08	0.36 ± 0.10
Brain	1.87 ± 0.31	1.22 ± 0.21	0.57 ± 0.07	0.28 ± 0.04	0.18 ± 0.04
Heart	12.4 ± 1.75	2.71 ± 0.49	1.58 ± 0.12	0.78 ± 0.12	0.53 ± 0.20
Liver	6.00 ± 1.00	13.5 ± 1.42	14.1 ± 1.57	11.4 ± 1.58	5.82 ± 1.90
Spleen	7.23 ± 0.86	11.5 ± 2.25	7.04 ± 0.86	3.39 ± 0.65	1.71 ± 0.65
Lung	29.9 ± 6.22	6.30 ± 1.44	4.16 ± 0.84	1.73 ± 0.24	1.07 ± 0.34
Kidney	25.2 ± 2.54	18.0 ± 2.35	11.2 ± 1.44	5.04 ± 0.69	3.53 ± 1.47
Pancreas	17.2 ± 3.84	28. 9 ± 7.44	41.2 ± 7.89	38.4 ± 8.03	48.5 ± 11.0
Muscle	3.53 ± 0.63	2.37 ± 0.29	1.54 ± 0.18	0.69 ± 0.14	0.61 ± 0.19
Bone	4.25 ± 0.73	6.39 ± 1.73	4.77 ± 1.72	3.55 ± 1.39	2.79 ± 0.70
Stomach[b]	2.62 ± 0.40	4.52 ± 1.45	3.45 ± 0.84	1.80 ± 0.54	2.51 ± 0.79
small intestine[b]	5.82 ± 1.30	13.4 ± 2.90	17.5 ± 4.44	16.8 ± 6.63	28.9 ± 8.03
Brain/Blood	1.22 ± 0.20	1.92 ± 0.23	1.14 ± 0.39	0.76 ± 0.18	0.51 ± 0.09

[a]Data are means of % ID/g of tissue ± SD, n = 5.

[b]Percentage of injected dose per organ.

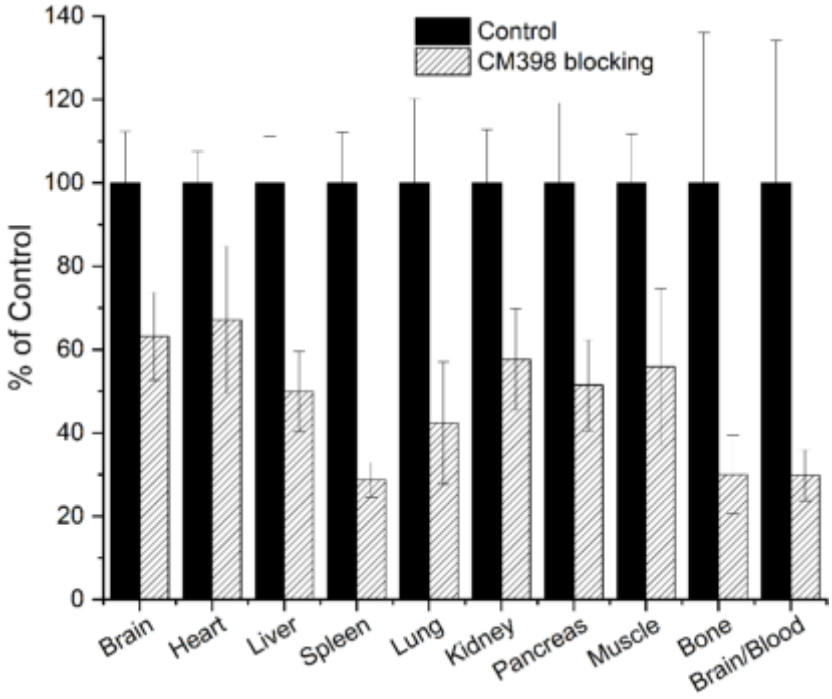

Figure 3. The effects of pre-administration with CM398 (5 μmol/kg) on biodistribution of [^{18}F]**1** at 30 min p.i. All values are means ± SD (n = 5 for each group). Student's *t* test (independent, two-tailed) was performed ($p < 0.01$).

Effect of P-gp on Radioligand Uptake in the Brain. Permeability-glycoprotein (P-gp) is an essential drug efflux transporter in the ATP family, which is expressed on the blood−brain barrier (BBB) and restricts penetration of drugs into the brain[44]. P-gp is also responsible for multidrug resistance in cancer chemotherapy and restricts drug entry into brain tumors[45-47]. To identify whether [^{18}F]**1** and [^{18}F]**4** are substrates for P-gp at the BBB, KM or ICR mice were treated with the P-gp inhibitor cyclosporine A (50 mg/kg, 0.1 mL)[48-50] at 60 min prior to radioligand injection. As shown in Figure 4 and Table S5, cyclosporine A significantly increased the accumulation of radioligands [^{18}F]**1** and [^{18}F]**4** in the brain by 336% ($p < 0.001$) and 370% ($p < 0.001$), respectively, at 2 min postinjection. Moreover, the brain-to-blood ratios were also significantly increased by 181% and 389% for [^{18}F]**1** ($p < 0.05$) and [^{18}F]**4** ($p < 0.001$), respectively. These findings suggest that both [^{18}F]**1** and [^{18}F]**4** are P-gp substrates.

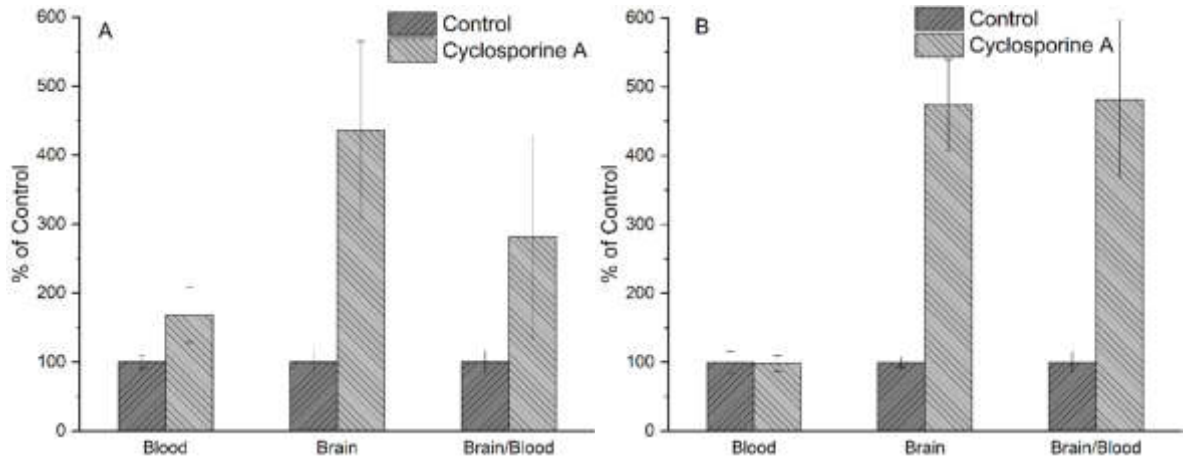

Figure 4. Effect of P-gp on brain uptake of [^{18}F]**1** (A) and [^{18}F]**4** (B) in mice. Student's *t* test (independent, two-tailed) was performed, $p < 0.05$ ([^{18}F]**1**) and $p < 0.001$ ([^{18}F]**4**) for the brain and brain-to-blood ratio (n = 5).

Micro-PET/CT Imaging in Rats. Given the good brain uptake and high specific binding of [^{18}F]**1** in mice, micro-PET/CT imaging experiment was conducted in anaesthetized Sprague−Dawley (SD) rats to further investigate its kinetics and specific binding *in vivo*. After administration of [^{18}F]**1**, dynamic PET scan was acquired for 90 min. The results are presented in Figures 5 and S6–S7. Radioactivity level in the brain reached peak rapidly and then washed out with time. Radiotracer accumulation in the blood, heart and lungs exhibited a sharp rise and then decreased rapidly. On the other hand, liver uptake increased with time, suggesting hepatic-intestinal metabolism of [^{18}F]**1** in rats.

Pretreatment of rats with CM398 (5 μmol/kg) at 5 min prior to radiotracer injection led to significantly decreased uptake in the brain and liver, indicating specific binding of [^{18}F]**1** to the σ_2 receptors in these organs. On the other hand, uptake levels in the blood, heart and lungs exhibited sharp rise and then decrease in a pattern similar to that in the baseline scans.

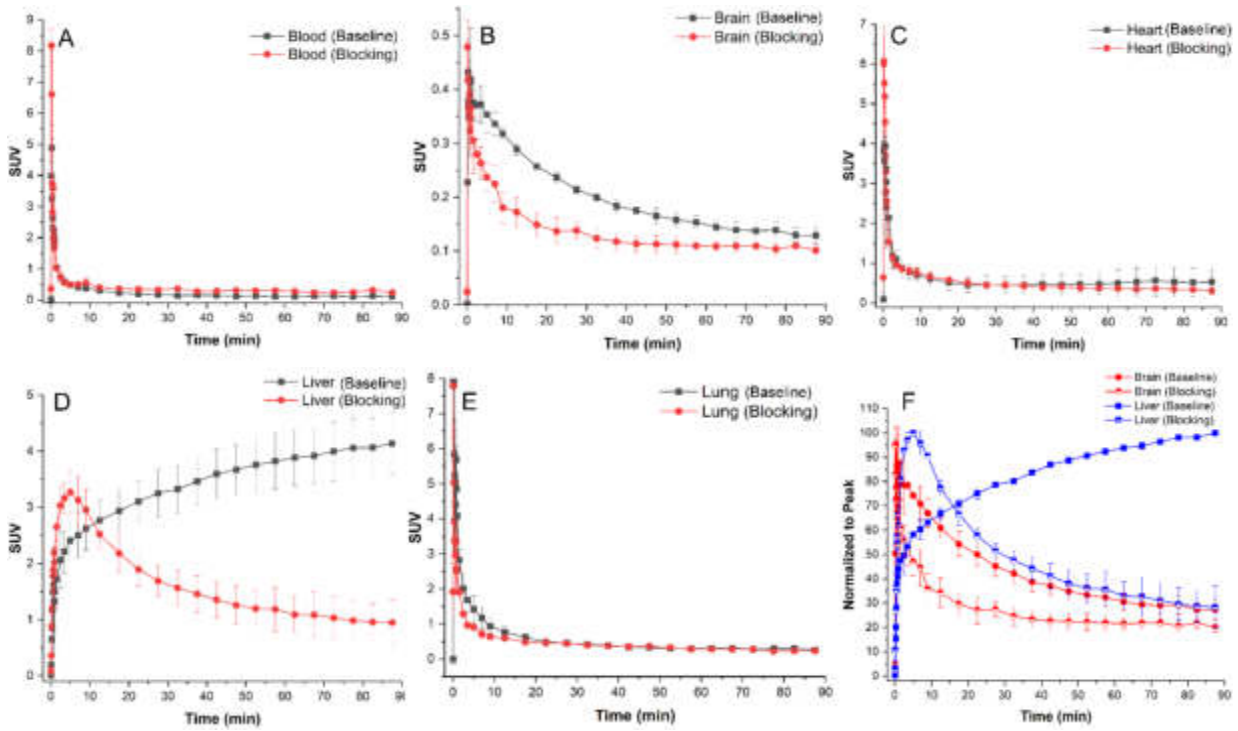

Figure 5. Time–activity curves (TACs) of [^{18}F]**1** in the blood (A), brain (B), heart (C), liver (D) and lung (E) from baseline (n = 3) and CM398 (5 μmol/kg) blocking scans (n = 3) in SD rats and TACs of [^{18}F]**1** in the brain and liver normalized to peak (F). SUV = standardized uptake value.

Micro-PET/CT Imaging in Balb/c Nude Mice Bearing U87MG Glioma Xenografts. To investigate potential application of [^{18}F]**1** in brain tumor imaging, static micro-PET/CT imaging were performed in Balb/c nude mice bearing U87MG glioma xenografts at different time points after injection (30, 60 and 120 min). Presented in Figures 6 and S8 are the static micro-PET/CT images from the baseline and CM398 (5 μmol/kg) blocking scans of [^{18}F]**1** in U87MG xenograft models. The detailed statistical data are provided in Table S6. The U87MG glioma xenografts were clearly visualized at 30, 60 and 120 min after radiotracer injection. High accumulation of radiotracer was observed in the tumor (n = 2) at 30 min and washed out gradually with time. The tumor SUV_{max} values were 1.14 ± 0.13, 0.96 ± 0.14 and 0.94 ± 0.12, respectively, at 30, 60 and 120 min, while SUV_{max} values in the muscle were 0.32 ± 0.07, 0.27 ± 0.05 and 0.25 ± 0.06, respectively, resulting in high tumor-to-muscle ratios ($SUV_{max\ (tumor)}$ / $SUV_{max\ (muscle)}$, T/M) of 3.58 ± 0.36, 3.63 ± 0.19 and 3.75 ± 0.37 at 30, 60 and 120 min, respectively.

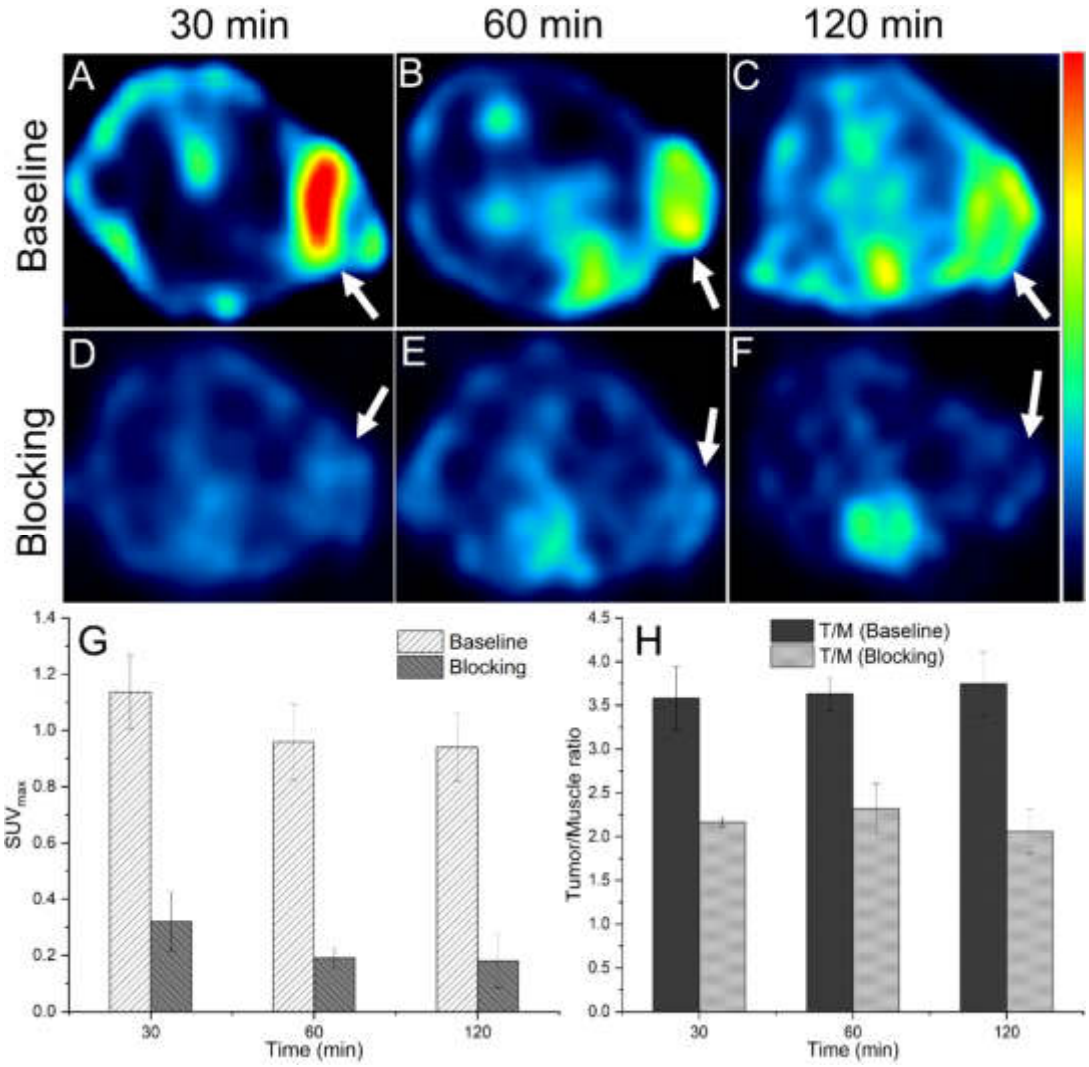

Figure 6. Static micro-PET/CT images from baseline and CM398 (5 μmol/kg) blocking scans of [^{18}F]**1** in U87MG xenograft model, summed from 30 to 40 min (A and D), 60–70 min (B and E) and 120–130 min (C and F) post-injection. The SUV_{max} values in tumor and the tumor/muscle ratio (T/M) are shown in G and H. SUV = standardized uptake value.

Injection of CM398 (5 μmol/kg body weight) prior to radioligand administration led to significantly decreased accumulation in the xenograft (SUV_{max}, n = 2) by 72% (30 min, p = 0.02), 80% (60 min, p = 0.02) and 81% (120 min, p = 0.02), indicating highly specific binding of [^{18}F]**1** to the σ_2 receptors in the U87MG tumor *in vivo*.

DISCUSSION

Increasing evidence has demonstrated that the σ_2 receptor plays a pivotal role in cancer biology and serves as a biomarker for the proliferative status of solid tumors[17-19]. Some recent research has been focused on a new cancer therapeutic mechanism *via* a novel regulation of cholesterol homeostasis mediated by the σ_2 receptors/TMEM97, such as controlling the trafficking of cholesterol via formation of a σ_2 receptor/TMEM97-PGRMC1-LDLR complex, and BRD2/SREBP2 cooperative regulation of the σ_2 receptor transcription in response to cholesterol deprivation[5, 51]. Recently, the σ_2 receptor/TMEM97 has been proposed as a potential therapeutic target in many human cancers[52]. The σ_2 receptor/TMEM97 expression appeared to be associated with the oncogenic potential of glioma and suppression of its expression can inhibit cancer cell growth and metastasis[22, 52]. Availability of suitable σ_2 receptor radioligands together with noninvasive PET imaging may monitor the progress of these human cancers and help understand this unique therapeutic mechanism associated with cholesterol homeostasis. However, the only σ_2 receptor PET probe in clinical trials for tumor imaging is [^{18}F]ISO-1[19, 20], which exhibits moderate affinity and low subtype selectivity[32-34]. An imaging probe with improved affinity and specificity for the σ_2 receptors will be advantageous for tumor imaging applications. Our aim in the current study is to develop a suitable radioligand for imaging the σ_2 receptors/TMEM97 in brain tumor.

In the current study we designed and synthesized a series of novel compounds as σ_2 receptor ligands. Among the benzimidazolone- (**1**–**2**), benzimidazole- (**3**–**6**) and benzene-based (**7**–**14**) derivatives, compounds **1**–**2** and **7**–**14** (except for compound **11**) with the 6,7-dimethoxy-1,2,3,4-tetrahydroisoquinoline pharmacophore exhibited nanomolar affinity, while compounds **3**–**6** possessed moderate affinity for the σ_2 receptors. In molecular docking studies, the receptor-ligand docking scores of compounds **1**–**4**, **7** and **12** with the σ_2 receptor crystal are in good agreement with their affinity for the σ_2 receptor. Similar to the binding mode of other benzimidazolone derivatives reported recently[42], a salt bridge with Asp29, hydrogen bond interactions with Asp29 and Tyr150, and π interactions with Tyr150 and Tyr50 have also been observed in the σ_2 receptor-binding site of compounds **1** and **2**. Moreover, Asp56, Glu73, and Gln77 appear to play important roles for the

binding of the σ_2 receptor to compounds reported here based on the mode analysis of molecular docking, consistent with the crucial amino acid residues identified initially[4].

Considering the affinity and lipophilicity, we selected compounds **1** and **4** for radiolabeling and evaluation of their *in vivo* kinetic and binding profiles, as well as the potential for tumor imaging application. Radioligand [^{18}F]**1** was prepared in good radiochemical yield and high radiochemical purity. Both radioligands [^{18}F]**1** (log$D_{7.4}$ = 1.78) and [^{18}F]**4** (log$D_{7.4}$ = 1.56) exhibited lower lipophilicity than [^{18}F]ISO-1 (log $D_{7.4}$ = 3.06)[33], which may lead to higher tissue uptake and binding specificity *in vivo*. In biodistribution studies in mice, radioligand [^{18}F]**1** exhibited higher brain uptake (1.87% ID/g, 2 min) than [^{18}F]ISO-1 (0.76% ID/g, 5 min)[33]. Pretreatment with CM398 led to significantly reduced accumulation of [^{18}F]**1** in organs known to contain the σ_2 receptors, indicating high specific binding of [^{18}F]**1** to the σ_2 receptors *in vivo*. For radioligand [^{18}F]**4**, remarkable reduction in uptake level was observed only in the pancreas, indicating that radioligand with moderate affinity provides measurable σ_2 specific binding only in organs with high expression of the σ_2 receptors. Pre-injection of cyclosporine A led to much higher accumulation of [^{18}F]**1** and [^{18}F]**4** at 2 min, suggesting that both [^{18}F]**1** and [^{18}F]**4** are P-gp substrates.

Glioblastoma is the most common malignant brain tumor with poor prognosis under the current standard treatment[53]. The diagnosis and treatment of glioma is very challenging. The U87MG tumor model is derived from human glioblastoma-astrocytoma cells and has been used to investigate anticancer potential of σ_2 receptor agonist[54]. Small animal PET/CT static imaging of [^{18}F]**1** demonstrated high uptake and clear visualization of U87MG glioma xenografts in nude mice with SUV_{max} values 1.14 ± 0.13, 0.96 ± 0.14 and 0.94 ± 0.12 at 30, 60 and 120 min, respectively, indicating better retention of [^{18}F]**1** in tumor (U87MG, tumor uptake$_{120min}$/tumor uptake$_{30\ min}$ = 0.82) than [^{18}F]ISO-1 (EMT-6, tumor uptake$_{120min}$/tumor uptake$_{30\ min}$ = 0.25)[33]. Moreover, [^{18}F]**1** (U87MG, tumor-to-muscle = 4, 120 min) exhibited higher tumor-to-muscle ratio than [^{18}F]ISO-1 (EMT-6, tumor-to-muscle = 3, 120 min)[33]. Co-injection of CM398 (5 μmol/kg) led to remarkable reduction of tumor uptake by 72%, 80%, and 81% at 30, 60 and 120 min, respectively, indicating high specific binding of [^{18}F]**1** to the σ_2 receptors in U87MG glioma xenografts. These findings demonstrated that

radioligand [^{18}F]**1** warrants further investigation as a highly specific σ_2 receptor probe for imaging the proliferative status of brain tumors.

Currently, the identities of the radioactive species in the tumor have not been fully elucidated. To further explore the applications of radioligand [^{18}F]**1**, micro-PET/CT imaging needs to be performed in U87MG and other orthotopic brain tumor models. These further investigations are in progress to evaluate [^{18}F]**1** as a candidate radioligand for imaging the proliferative status of brain tumors.

CONCLUSIONS

A series of hydrophilic benzimidazolone-, benzimidazole-, and benzene-based derivatives with 6,7-dimethoxy-1,2,3,4-tetrahydroisoquinoline or 5,6-dimethoxyisoindoline pharmacophore have been designed and synthesized. Compound **1** was found to possess nanomolar affinity for the σ_2 receptors, high subtype selectivity and high selectivity over other 40 receptors or transporters. The corresponding radioligand [^{18}F]**1** was prepared and found to exhibit high specific binding to the σ_2 receptors in rodent organs known to express σ_2 receptors. Moreover, small animal PET/CT imaging studies with [^{18}F]**1** demonstrated high tumor uptake and clear visualization of U87MG glioma xenografts in nude mice. In particular, [^{18}F]**1** possessed very high specific binding to the σ_2 receptors in U87MG xenografts. These findings demonstrated that radioligand [^{18}F]**1**, with appropriate lipophilicity, nanomolar affinity for the σ_2 receptors and high selectivity *in vitro*, high tumor uptake and σ_2 receptor specific binding in U87MG glioma xenografts, warrants further investigation as a potential σ_2 receptor probe for imaging the proliferative status in brain tumors.

EXPERIMENTAL SECTION

General. All chemical reagents and solvents for synthesis and radiolabeling were directly obtained from commercial resources and used without further purification. Column chromatography on silica gel was utilized to purify intermediates and target compounds, and thin-layer chromatography (TLC) to monitor the progress of reactions using 0.25 mm silica gel on aluminum plates. NMR spectra (^{1}H,

^{13}C and ^{19}F), mass spectrometry (MS) and high-resolution mass spectrometry (HRMS) were obtained and handled in a manner similar to that reported previously[37, 55]. NMR spectra were obtained on a JEOL spectrometer (400 or 600 MHz for ^{1}H, 100 or 150 MHz for ^{13}C, 375 or 565 MHz for ^{19}F) in $CDCl_3$ or DMSO-d_6 at room temperature. Chemical shifts (δ) are reported in parts per million (ppm) with tetramethylsilane (TMS) as internal standard, and coupling constants (*J*) are reported in Hertz (Hz). The multiplicities are abbreviated as follows: s = singlet, d = doublet, t = triplet, q = quartet, m = multiplet, br = broad signal, dd = doublet of doublets, dt = doublet of triplets, td = triplet of doublets, and ddd = doublet of doublet of doublets. HPLC methods were used to determine the purity of the compounds used in binding assays. All target compounds are > 95% pure by HPLC analysis (Supporting Information).

The molecular docking was conducted with the Schrödinger software by referencing the reported methods[4]. The available protein crystal structures (PDB code: 7MFI) was directly obtained from ProteinDataBank (www.rcsb.org). ^{18}F was produced by the $^{18}O(p,n)^{18}F$ reaction with an cyclotron (HM-20, Sumitomo, Japan). Purification and analysis of radioligands were carried out using a Shimadzu SCL-20 AVP HPLC system (Shimadzu Corp., Japan) with a ReproSil-Pur Basic-C18 column (Dr. Maisch Gmbh, Germany). The detailed information is provided in the Supporting Information. Normal KM mice (20 ± 2 g, 4–5 weeks), ICR mice (20 ± 2 g, 4–5 weeks) and male SD rats (200 ± 10 g, 6–7 weeks) were purchased from Vital River Experimental Animal Technical Co., Ltd. All procedures related to the animal experiments were performed in compliance with relevant laws and institutional guidelines and approved by the Institutional Animal Care and Use Committee of Beijing Normal University.

Chemistry

Tert-Butyl 2-oxo-2,3-dihydro-1H-benzo[d]imidazole-1-carboxylate (**16**). Sodium hydride (NaH, 288 mg, 12 mmol) was added portion wise to a stirred solution of 1*H*-benzo[d]imidazol-2(3*H*)-one (**15**, 1,341 mg, 10 mmol) in anhydrous DMF (20 mL) at room temperature. After 5 min, a solution of di-*tert*-butyl dicarbonate ($(Boc)_2O$, 2,183 mg, 11 mmol) in dry DMF (20 mL) was added dropwise. The mixture was stirred at room temperature for 12 h, then treated with water (50 mL) and extracted with CH_2Cl_2 (3 × 10 mL). The combined extracts were washed with water, and dried over anhydrous

Na_2SO_4. The solvent was removed under reduced pressure, and the residue diluted with saturated NH_4Cl solution and extracted with CH_2Cl_2 (3 × 10 mL). The combined organic phase was dried over anhydrous Na_2SO4, filtered and concentrated. The residue was purified by flash column chromatography over silica gel using a mixture of hexane and EtOAc (2:1) as eluent to furnish compound **16** as a white solid (92 %). ^{1}H NMR (400 MHz, $CDCl_3$): δ 10.56 (s, 1H), 7.71 (d, *J* = 7.9 Hz, 1H), 7.18 – 7.05 (m, 3H), 1.70 (s, 9H). ESI–MS calcd for $C_{12}H_{15}N_2O_3$ $[M + H]^+$ *m*/*z* 235.11; found *m*/*z* 235.10.

Tert-Butyl 3-(4-bromobutyl)-2-oxo-2,3-dihydro-1H-benzo[d]imidazole-1-carboxy-late (**17**). To a solution of intermediate **16** (468 mg, 2 mmol) in DMF (10 mL) were added K_2CO_3 (553 mg, 4 mmol), TEA (405 mg, 4 mmol) and 1,4-dibromobutane (432 mg, 2 mmol). The mixture was stirred at 60 °C for 12 h followed by treatment with water (50 mL) and extraction with CH_2Cl_2 (3 × 10 mL). The combined extracts were washed with water, dried over anhydrous Na_2SO_4, and concentrated. The solvent was removed under reduced pressure, followed by dilution with saturated NH_4Cl solution and extraction with CH_2Cl_2 (3 × 10 mL). The combined organic phase was dried over anhydrous Na_2SO4, filtered and concentrated. The residue was purified by flash column chromatography over silica gel using a mixture of hexane and EtOAc (1:1) as eluent to furnish compound **17** as a yellowish oil (56 %). ^{1}H NMR (600 MHz, $CDCl_3$): δ 7.83 (d, *J* = 7.5 Hz, 1H), 7.21 – 7.18 (m, 1H), 7.12 (td, *J* = 7.9, 1.2 Hz, 1H), 6.98 (d, *J* = 7.9 Hz, 1H), 3.92 – 3.86 (m, 2H), 3.47 – 3.42 (m, 2H), 1.95 – 1.91 (m, 4H), 1.67 (s, 9H). ESI–MS calcd. for $C_{16}H_{22}BrN_2O_3$ $[M + H]^+$ *m*/*z* 369.08; found *m*/*z* 369.09.

Tert-Butyl 3-(4-(6,7-dimethoxy-3,4-dihydroisoquinolin-2(1H)-yl)butyl)-2-oxo-2,3-dihydro-1H-benzo[d]imidazole-1-carboxylate (**18**). To a solution of intermediate **17** (411 mg, 1.2 mmol) in MeCN (20 mL) were added K_2CO_3 (332 mg, 2.4 mmol), TEA (243 mg, 2.4 mmol) and 6,7-dimethoxy-1,2,3,4-tetrahydroisoquinoline (288 mg, 1.25 mmol). The mixture was refluxed for 12 h. After filtration, the solvent was removed under reduced pressure. The residue was then treated with water (20 mL) and extracted with CH_2Cl_2 (3 × 10 mL). The combined extracts were washed with water, dried over anhydrous Na_2SO_4, and concentrated. The crude product was purified by flash chromatography (EtOAc/hexane/TEA/MeOH = 20/20/1/1) to yield compound **18** as a white solid (53 %).^{1}H NMR (600

MHz, $CDCl_3$): δ 7.81 (d, *J* = 7.6 Hz, 1H), 7.14 (d, *J* = 7.7 Hz, 1H), 7.10 (t, *J* = 7.8 Hz, 1H), 6.98 (d, *J* = 8.0 Hz, 1H), 6.58 (s, 1H), 6.50 (s, 1H), 3.90 (t, *J* = 7.2 Hz, 2H), 3.83 (d, *J* = 3.3 Hz, 6H), 3.56 (s, 2H), 2.82 (t, *J* = 5.9 Hz, 2H), 2.72 (s, 2H), 2.57 (s, 2H), 1.84 (m, 2H), 1.69 – 1.67 (m, 11H). ESI–MS calcd. for $C_{27}H_{36}N_3O_5$ $[M + H]^+$ *m*/*z* 482.26; found *m*/*z* 482.26.

1-(4-(6,7-Dimethoxy-3,4-dihydroisoquinolin-2(1H)-yl)butyl)-1,3-dihydro-2H-benzo[d]imidazol-2-one (**19**). To a solution of intermediate **18** (1,169 mg, 2.43 mmol) in CH_2Cl_2 (10 mL) was added TFA (2 mL). The mixture was stirred at room temperature for 1 h. After filtration, the solvent was removed under reduced pressure. The residue was then treated with water (20 mL) and saturated $NaHCO_3$ solution (10 mL) and extracted with CH_2Cl_2 (3 × 10 mL). The combined extracts were washed with water, dried over anhydrous Na_2SO_4, and concentrated. The crude product was purified by flash chromatography (EtOAc/hexane/TEA/MeOH = 20/10/1/1) to yield compound **19** as a white solid (93%). ^{1}H NMR (400 MHz, $CDCl_3$): δ 9.46 (s, 1H), 7.12 – 6.97 (m, 4H), 6.57 (s, 1H), 6.49 (s, 1H), 3.94 (t, *J* = 7.1 Hz, 2H), 3.82 (d, *J* = 5.7 Hz, 6H), 3.55 (s, 2H), 2.80 (t, *J* = 5.9 Hz, 2H), 2.71 (d, *J* = 5.7 Hz, 2H), 2.57 (t, *J* = 7.4 Hz, 2H), 1.86 (m, 2H), 1.70 (q, *J* = 8.2 Hz, 2H). ESI–MS calcd. for $C_{22}H_{28}N_3O_3$ $[M + H]^+$ *m*/*z* 382.21; found *m*/*z* 382.23.

1-(4-(6,7-Dimethoxy-3,4-dihydroisoquinolin-2(1H)-yl)butyl)-3-(2-fluoroethyl)-1,3-dihydro-2H-benzo[d]imidazol-2-one (**1**). To a solution of intermediate **19** (241 mg, 0.64 mmol) in DMF (10 mL) were added K_2CO_3 (355 mg, 2.5 mmol), 1-bromo-2-fluoroethane (190 mg, 1.25 mmol) and tetrabutylammonium iodide (TBAI, 48 mg, 20% mmol). The mixture was refluxed for 12 h. After filtration, the solvent was removed under reduced pressure. The residue was then treated with water (20 mL) and extracted with CH_2Cl_2 (3 × 10 mL). The combined extracts were washed with water, dried over anhydrous Na_2SO_4, and concentrated. The crude product was purified by flash chromatography (EtOAc/hexane/TEA/MeOH = 20/20/1/1) to yield compound **1** as a yellowish solid (58%). M.P.: 78.3–81.1 °C. ^{1}H NMR (600 MHz, $CDCl_3$): δ 7.09 – 7.05 (m, 3H), 7.03 – 7.01 (m, 1H), 6.58 (s, 1H), 6.50 (s, 1H),4.71 (dt, *J* = 47.1, 4.9 Hz, 2H), 4.18 (dt, *J* = 26.1, 4.9 Hz, 2H), 3.95 – 3.93 (m, 2H), 3.84 (s, 3H), 3.83 (s, 3H), 3.53 (s, 2H), 2.80 (s, 2H), 2.69 (s, 2H), 2.55 (s, 2H), 1.85 (q, *J* = 7.5 Hz, 2H), 1.75 – 1.60 (m, 2H). ^{19}F NMR (565 MHz, $CDCl_3$): δ -220.74. ^{13}C NMR (150 MHz, $CDCl_3$):

δ 154.21, 147.62, 147.31, 129.77, 129.42, 121.50, 121.37, 111.43, 109.57, 108.25, 107.90, 82.33 (d, *J* = 171.5 Hz), 57.60, 56.01, 55.99, 55.75, 51.05, 41.81 (d, *J* = 21.8 Hz), 41.06, 28.66, 26.31, 24.40, 15.36. HR-MS calcd. for $C_{24}H_{31}N_3O_3F$ $[M + H]^+$ *m*/*z* 428.2343; found *m*/*z* 428.2347.

2-(3-Fluoro-4-nitrophenoxy)tetrahydro-2H-pyran (**21**). To a solution of substrate **20** (3,142 mg, 20 mmol) in CH_2Cl_2 (20 mL) were added 3,4-dihydro-2*H*-pyran (DHP, 4,206 mg, 50 mmol) and TFA (456 mg, 20% mmol, 0.31 mL). The mixture was stirred at room temperature for 2 h. After filtration, the solvent was removed under reduced pressure. The residue was then treated with water (20 mL) and saturated $NaHCO_3$ solution (10 mL) and extracted with CH_2Cl_2 (3 × 10 mL). The combined extracts were washed with water, dried over anhydrous Na_2SO_4, and concentrated. The crude product was purified by flash chromatography (EtOAc/hexane = 20/1) to yield compound **21** as a yellowish solid (98%). ^{1}H NMR (400 MHz, $CDCl_3$): δ 8.06 (td, *J* = 9.2, 5.7 Hz, 1H), 6.99 – 6.85 (m, 2H), 5.51 (t, *J* = 3.0 Hz, 1H), 3.78 (td, *J* = 11.0, 3.0 Hz, 1H), 3.68 – 3.63 (m, 1H), 1.91 – 1.87 (m, 2H), 1.77 – 1.69 (m, 2H), 1.65 – 1.59 (m, 2H). ESI–MS calcd. for $C_{11}H_{13}FNO_4$ $[M + Na]^+$ *m*/*z* 242.06; found *m*/*z* 242.06.

N-Methyl-2-nitro-5-((tetrahydro-2H-pyran-2-yl)oxy)aniline (**22**). The procedure for the synthesis of **22** was referenced to literature[39] and obtained as a yellowish oil (81%). ^{1}H NMR (400 MHz, $CDCl_3$): δ 8.21 (s, 1H), 8.13 (dd, *J* = 9.2, 3.9 Hz, 1H), 6.43 – 6.31 (m, 2H), 5.54 (t, *J* = 3.1 Hz, 1H), 3.90 – 3.78 (m, 1H), 3.67 – 3.62 (m, 1H), 2.99 (s, 3H), 2.02 – 1.96 (m, 1H), 1.90 – 1.86 (m, 2H), 1.74 – 1.67 (m, 2H), 1.64 – 1.59 (m, 1H). ESI–MS calcd. for $C_{12}H_{17}N_2O_4$ $[M + H]^+$ *m*/*z* 253.12; found *m*/*z* 253.12.

N^1-Methyl-5-((tetrahydro-2H-pyran-2-yl)oxy)benzene-1,2-diamine (**23**). The procedure for the synthesis of **23** was referenced to literature[39] and obtained as a brownish oil (83%). ^{1}H NMR (400 MHz, $CDCl_3$): δ 6.63 (d, *J* = 8.2 Hz, 1H), 6.39 (s, 2H), 5.32 (t, *J* = 3.4 Hz, 1H), 3.97 (ddd, *J* = 12.0, 9.1, 3.2 Hz, 1H), 3.62 – 3.56 (m, 1H), 3.22 (s, 3H), 2.84 (s, 3H), 2.09 – 1.91 (m, 1H), 1.89 – 1.79 (m, 2H), 1.74 – 1.53 (m, 3H). ESI–MS calcd. for $C_{12}H_{19}N_2O_2$ $[M + H]^+$ *m*/*z* 223.14; found *m*/*z* 223.16.

1-Methyl-5-((tetrahydro-2H-pyran-2-yl)oxy)-1,3-dihydro-2H-benzo[d]imidazol-2-one (**24**). The procedure for the synthesis of **24** was referenced to literature[39] and obtained as a white solid (32%). ^{1}H NMR (600 MHz, DMSO-d_6): δ 7.49 (d, *J* = 8.6 Hz, 1H), 7.04 (d, *J* = 2.3 Hz, 1H), 6.86 (dd,

J = 8.7, 2.4 Hz, 1H), 5.54 (q, *J* = 3.2 Hz, 1H), 3.80 (ddd, *J* = 11.1, 9.3, 3.4 Hz, 1H), 3.59 – 3.56 (m, 1H), 3.29 (s, 3H), 1.95 – 1.73 (m, 3H), 1.66–1.54 (m, 3H). ESI–MS calcd. for $C_{13}H_{17}N_2O_3$ $[M + H]^+$ *m*/*z* 249.12; found *m*/*z* 249.21.

3-(4-Bromobutyl)-1-methyl-5-((tetrahydro-2H-pyran-2-yl)oxy)-1,3-dihydro-2H-benzo[d]imidazol-2-one (**25**). The procedure for the synthesis of **17** was applied to intermediate **24** (250 mg, 1 mmol) with K_2CO_3 (553 mg, 4 mmol), tetrabutylammonium iodide TBAI (74 mg, 20% mmol) and 1-bromo-2-fluoroethane (260 mg, 1.2 mmol) in DMF (10 mL) to afford compound **25** as a colorless oil (58%). ^{1}H NMR (400 MHz, DMSO-d_6): δ 7.09 (d, *J* = 8.5 Hz, 1H), 6.91 (d, *J* = 2.3 Hz, 1H), 6.76 (dd, *J* = 8.5, 2.3 Hz, 1H), 5.43 (t, *J* = 3.3 Hz, 1H), 3.85 – 3.79 (m, 3H), 3.58 – 3.52 (m, 3H), 3.29 (s, 3H), 1.93 – 1.86 (m, 1H), 1.82 – 1.81 (m, 6H), 1.66 – 1.53 (m, 3H). ESI–MS calcd for $C_{17}H_{24}BrN_2O_3$ $[M + H]^+$ *m*/*z* 383.10; found *m*/*z* 383.10.

3-(4-(6,7-Dimethoxy-3,4-dihydroisoquinolin-2(1H)-yl)butyl)-5-hydroxy-1-methyl-1,3-dihydro-2H-benzo[d]imidazol-2-one (**27**). To a solution of intermediate **25** (246 mg, 0.65 mmol) in MeCN (10 mL) were added K_2CO_3 (346 mg, 2.5 mmol), TEA (253 mg, 2.5 mmol) and 6,7-dimethoxy-1,2,3,4-tetrahydroisoquinoline (184 mg, 0.8 mmol). The mixture was refluxed for 12 h. After filtration, the solvent was removed under reduced pressure. The residue was then treated with water (20 mL) and extracted with CH_2Cl_2 (3 × 10 mL). The solvents were evaporated and the crude product **26** was dissolved in MeOH (10 mL) followed by addition of HCl solution (1 M in MeOH). The mixture was stirred at room temperature for 1 h, then treated with water (20 mL), and $NH_3{\cdot}H_2O$ to pH > 8, and extracted with CH_2Cl_2 (3 × 10 mL). The combined extracts were washed with water, dried over anhydrous Na_2SO_4, and concentrated. The crude product was purified by silica gel column chromatography (EtOAc/hexane/TEA/MeOH = 20/10/3/1) to yield compound **27** as a white solid (98%). ^{1}H NMR (400 MHz, DMSO-d_6): δ 9.07 (s, 1H), 6.94 (d, *J* = 8.4 Hz, 1H), 6.63 (s, 1H), 6.59 (s, 1H), 6.54 (d, *J* = 2.3 Hz, 1H), 6.44 (dd, *J* = 8.4, 2.3 Hz, 1H), 3.78 (t, *J* = 7.0 Hz, 2H), 3.69 (d, *J* = 2.5 Hz, 6H), 3.40 (s, 2H), 3.24 (s, 3H), 2.67 (t, *J* = 5.7 Hz, 2H), 2.56 (t, *J* = 7.2 Hz, 2H), 2.42 (t, *J* = 7.1 Hz, 2H), 1.70 – 1.62 (m, 2H), 1.53 – 1.46 (m, 2H). ESI–MS calcd. for $C_{23}H_{30}N_3O_4$ $[M + H]^+$ *m*/*z* 412.22; found *m*/*z* 412.23.

3-(4-(6,7-Dimethoxy-3,4-dihydroisoquinolin-2(1H)-yl)butyl)-5-(2-fluoroethoxy)-1-methyl-1,3-dihydro-2H-benzo[d]imidazol-2-one (**2**). The procedure for the synthesis of **1** was applied to intermediate **27** (103 mg, 0.25 mmol) with K_2CO_3 (138 mg, 1 mmol), TEA (50 mg, 0.5 mmol) and 1-bromo-2-fluoroethane (64 mg, 0.5 mmol) in MeCN (10 mL) to afford compound **2** as a white solid (51%). M.P.: 38.8–41.5 °C. ^{1}H NMR (600 MHz, $CDCl_3$): δ 6.88 – 6.87 (m, 1H), 6.63 (d, *J* = 7.7 Hz, 2H), 6.58 (s, 1H), 6.50 (s, 1H), 4.80 – 4.78 (m, 1H), 4.72 – 4.70 (m, 1H), 4.25 – 4.23 (m, 1H), 4.20 – 4.19 (m, 1H), 3.91 – 3.88 (m, 2H), 3.83 (d, *J* = 4.0 Hz, 6H), 3.55 (s, 2H), 3.37 (s, 3H), 2.81 (s, 2H), 2.72 (s, 2H), 2.56 (s, 2H), 1.85 – 1.80 (m, 2H), 1.68 – 1.67 (m, 2H). ^{19}F NMR (565 MHz, $CDCl_3$): δ -223.64. ^{13}C NMR (150 MHz, $CDCl_3$): δ 154.82, 154.24, 147.63, 147.31, 131.06, 124.10, 111.44, 109.58, 107.92, 107.33, 96.26, 82.10 (d, *J* = 170.7 Hz), 68.43 (d, *J* = 20.4 Hz), 57.56, 55.99 (d, *J* = 4.8 Hz), 55.69, 50.99, 41.03, 29.77, 28.58, 27.22, 26.36, 24.32. HR–MS calcd. for $C_{25}H_{33}FN_3O_4$ $[M + H]^+$ *m*/*z* 458.2449; found *m*/*z* 458.2465.

1H-benzo[d]imidazol-6-ol (**31**). Compound **29** (4,500 mg, 15.3 mmol) was added to 48% aqueous HBr solution (20 mL). The mixture was stirred at 110 °C for 6 h, cooled in ice-water, treated with water (20 mL) and $NH_3{\cdot}H_2O$ to pH > 8, then extracted with CH_2Cl_2 (3 × 10 mL). Purification by flash chromatography on silica gel (CH_2Cl_2/MeOH = 10/1) yielded compound **31** as a white solid (51%). ^{1}H NMR (600 MHz, DMSO-d_6): δ 12.08 (s, 1H), 9.04 (s, 1H), 7.97 (s, 1H), 7.33 (d, *J* = 8.6 Hz, 1H), 6.83 (s, 1H), 6.63 (dd, *J* = 8.6, 1.7 Hz, 1H). ESI–MS calcd. for $C_7H_7N_2O$ $[M + H]^+$ *m*/*z* 135.06; found *m*/*z* 135.05.

5-((tert-Butyldimethylsilyl)oxy)-1H-benzo[d]imidazole (**32**). To a solution of intermediate **30** (1,345 mg, 10 mmol) in CH_2Cl_2 (20 mL), were added imidazole (1,200 mg, 20 mmol) and *tert*-butyldimethylsilyl chloride (TBSCl, 4,206 mg, 50 mmol) in 0 °C. The mixture was stirred at room temperature for 2 h. After filtration, the solvent was removed under reduced pressure. The residue was treated with water (20 mL) and extracted with CH_2Cl_2 (3 × 10 mL). The combined extracts were washed with water, dried over anhydrous Na_2SO_4, and concentrated. The crude product was purified by flash chromatography on silica gel (CH_2Cl_2/MeOH = 20/1) to yield compound **32** as a yellowish solid (87%). ^{1}H NMR (400 MHz, $CDCl_3$): δ 8.40 (s, 1H), 8.01 (s, 1H), 7.51 (d, *J* = 8.7 Hz, 1H), 7.07

(d, *J* = 2.2 Hz, 1H), 6.84 (dd, *J* = 8.7, 2.3 Hz, 1H), 0.99 (s, 9H), 0.19 (s, 6H). ESI–MS calcd for $C_{13}H_{21}N_2OSi$ $[M + H]^+$ *m*/*z* 249.14; found *m*/*z* 249.13.

6-((tert-Butyldimethylsilyl)oxy)-1H-benzo[d]imidazole (**33**). The procedure for the synthesis of **32** was applied to intermediate **31** (1,350 mg, 10 mmol), imidazole (1,250 mg, 20 mmol) and TBSCl (4,200 mg, 50 mmol) in CH_2Cl_2 (10 mL) to afford compound **33** as a yellowish solid (85%). ^1H NMR (400 MHz, $CDCl_3$): δ 8.60 (s, 1H), 8.01 (s, 1H), 7.51 (d, *J* = 8.7 Hz, 1H), 7.07 (d, *J* = 2.2 Hz, 1H), 6.84 (dd, *J* = 8.7, 2.2 Hz, 1H), 0.99 (s, 9H), 0.19 (s, 6H). ESI–MS calcd for $C_{13}H_{21}N_2OSi$ $[M + H]^+$ *m*/*z* 249.14; found *m*/*z* 249.13.

Because intermediates **34**–**39** were unstable, they were subjected to the next step of synthesis after a rapid separation and purification.

To a solution of intermediate **32** or **33** (500 mg, 2 mmol) in DMF (20 mL) were added Cs_2CO_3 (326 mg, 1 mmol), NaI (75 mg, 20% mmol) and 1,4-dibromobutane (864 mg, 4 mmol). The mixture was stirred at 60 °C for 1 h, then treated with water (50 mL) and extracted with CH_2Cl_2 (3 × 10 mL). The combined extracts were washed with water, dried over anhydrous Na_2SO_4, and concentrated. The crude product was rapidly separated and purified by silica gel column chromatography (CH_2Cl_2/MeOH = 20/1) to obtain **34** or **35**. Intermediate **34** or **35** was then dissolved in MeCN (10 mL), followed by addition of K_2CO_3 (364 mg, 2.5 mmol), TEA (101 mg, 1 mmol) and substrate **S4** or 6,7-dimethoxy-1,2,3,4-tetrahydroisoquinoline (about 200 mg, 1 mmol). The mixture was refluxed for 12 h. After filtration, the solvent was removed under reduced pressure. The residue was then treated with water (20 mL) and extracted with CH_2Cl_2 (3 × 10 mL). The combined extracts were washed with water, dried over anhydrous Na_2SO_4, and concentrated. The crude product was dissolved in tetrabutylammonium fluoride solution (1 M in THF). The mixture was stirred at room temperature for 1 h, filtered and the solvent removed under reduced pressure. The residue was then treated with water (20 mL) and extracted with CH_2Cl_2 (3 × 10 mL). The combined extracts were washed with water, dried over anhydrous Na_2SO_4, and concentrated. The crude product was purified by silica gel column chromatography (EtOAc/hexane/MeOH/TEA = 5/1/1/0.1) to obtain intermediates **36**–**39**, which were used immediately for the next step of synthesis.

1-(4-(5,6-Dimethoxyisoindolin-2-yl)butyl)-6-(2-fluoroethoxy)-1H-benzo[d]imidazole (**3**). To a solution of intermediate **36** (370 mg, 1 mmol) in MeCN (10 mL) were added K_2CO_3 (360 mg, 2.5 mmol), TEA (100 mg, 1 mmol) and 1-bromo-2-fluoroethane (256 mg, 2 mmol). The mixture was refluxed for 12 h. After filtration, the solvent was removed under reduced pressure. The residue was then treated with water (20 mL) and extracted with CH_2Cl_2 (3 × 10 mL). The combined extracts were washed with water, dried over anhydrous Na_2SO_4, and concentrated. The crude product was purified by flash column chromatography on silica gel (CH_2Cl_2/MeOH = 10/1) to yield compound **3** as a greyish solid (32%). M.P.: 132.8–133.4 °C. ^{1}H NMR (400 MHz, $CDCl_3$): δ 7.84 (d, *J* = 16 Hz, 1H), 7.39 – 7.15 (m, 1H), 7.04 – 6.80 (m, 2H), 6.71 (s, 2H), 4.84 – 4.65 (m, 2H), 4.39 – 4.04 (m, 4H), 3.84 (d, *J* = 6.3 Hz, 10H), 2.74 (q, *J* = 7.4 Hz, 2H), 2.02 – 1.94 (m, 2H), 1.60 (q, *J* = 7.4 Hz, 2H). ^{19}F NMR (375 MHz, $CDCl_3$): δ -223.47. ^{13}C NMR (100 MHz, $CDCl_3$): δ 155.55, 148.64, 142.58, 138.99, 134.45, 131.21, 121.04, 113.85, 111.76, 110.31, 105.94, 103.66, 94.97, 82.11 (d, *J* = 170.6 Hz), 68.07 (dd, *J* = 20.5, 15.6 Hz), 59.22, 56.22, 55.19, 44.90, 27.40, 25.90. HR–MS calcd. for $C_{23}H_{29}FN_3O_3$ [M + H]$^+$ *m*/*z* 414.2187; found *m*/*z* 414.2189.

1-(4-(5,6-Dimethoxyisoindolin-2-yl)butyl)-5-(2-fluoroethoxy)-1H-benzo[d]imidazole (**4**). The procedure for the synthesis of **3** was applied to intermediate **37** (370 mg, 1 mmol), K_2CO_3 (360 mg, 2.5 mmol), TEA (100 mg, 1 mmol) and 1-bromo-2-fluoroethane (256 mg, 2 mmol) in MeCN (10 mL) to afford compound **4** as a yellowish solid (34%). M.P.: 118.1–119.3 °C. ^{1}H NMR (400 MHz, $CDCl_3$): δ 7.86 (d, *J* = 16 Hz, 1H), 7.30 – 7.25 (m, 2H), 7.01 – 6.90 (m, 1H), 6.71 (s, 2H), 4.85 – 4.79 (m, 1H), 4.73 – 4.67 (m, 1H), 4.30 – 4.25 (m, 1H), 4.23 – 4.16 (m, 3H), 3.99 (d, *J* = 8.6 Hz, 4H), 3.84 (s, 6H), 2.84 (q, *J* = 7.9 Hz, 2H), 2.04 – 1.95 (m, 2H), 1.74 – 1.64 (m, 2H). ^{19}F NMR (375 MHz, $CDCl_3$): δ -223.51. ^{13}C NMR (150 MHz, $CDCl_3$): δ 155.64, 149.10, 143.31, 142.54, 134.40, 128.91, 121.10, 113.94, 111.90, 110.27, 105.87, 103.72, 94.92, 82.69, 68.11 (dd, *J* = 30.9, 20.5 Hz), 59.08, 56.25, 55.35, 55.25, 45.05, 44.79, 27.63, 27.35. HR–MS calcd. for $C_{23}H_{29}FN_3O_3$ [M + H]$^+$ *m*/*z* 414.2187; found *m*/*z* 414.2190.

2-(4-(5-(2-Fluoroethoxy)-1H-benzo[d]imidazol-1-yl)butyl)-6,7-dimethoxy-1,2,3,4-tetrahydro-isoquinoline (**5**). The procedure for the synthesis of **3** was applied to intermediate **38** (368 mg, 1

mmol), K_2CO_3 (355 mg, 2.5 mmol), TEA (103 mg, 1 mmol) and 1-bromo-2-fluoroethane (266 mg, 2 mmol) in MeCN (10 mL) to afford compound **5** as a yellowish solid (40%). M.P.: 164.5–167.2 °C. ^{1}H NMR (600 MHz, $CDCl_3$): δ 7.84 (d, *J* = 23.4 Hz, 1H), 7.69 (d, *J* = 8.8 Hz, 1H), 7.30 – 7.26 (m, 1H), 6.99 (dd, *J* = 8.8, 2.4 Hz, 1H), 6.58 (s, 1H), 6.48 (d, *J* = 2.5 Hz, 1H), 4.83 – 4.70 (m, 2H), 4.29 – 4.16 (m, 4H), 3.83 (s, 3H), 3.82 (s, 3H), 3.59 (s, 2H), 2.83 (t, *J* = 5.5 Hz, 2H), 2.78 – 2.75 (m, 2H), 2.59 (q, *J* = 8.2, 7.7 Hz, 2H), 2.00 – 1.95 (m, 2H), 1.71 – 1.64 (m, 2H). ^{19}F NMR (565 MHz, $CDCl_3$): δ -223.59. ^{13}C NMR (100 MHz, $CDCl_3$): δ 155.60, 154.96, 147.97, 147.59, 143.33, 142.61, 138.97, 134.38, 128.88, 121.06, 113.89, 111.83, 111.42, 110.32, 109.48, 103.64, 94.97, 82.12 (d, *J* = 170.4 Hz), 68.09 (t, *J* = 20.7 Hz), 56.02 (d, *J* = 3.5 Hz), 50.78, 45.13, 44.91, 27.70, 27.46, 23.98 (d, *J* = 9.6 Hz). HR–MS calcd. for $C_{24}H_{31}FN_3O_3$ $[M + H]^+$ *m*/*z* 428.2344; found *m*/*z* 428.2347.

2-(4-(6-(2-Fluoroethoxy)-1H-benzo[d]imidazol-1-yl)butyl)-6,7-dimethoxy-1,2,3,4-tetrahydro-isoquinoline (**6**). The procedure for the synthesis of **3** was applied to intermediate **39** (360 mg, 1 mmol), K_2CO_3 (364 mg, 2.5 mmol), TEA (105 mg, 1 mmol) and 1-bromo-2-fluoroethane (278 mg, 2 mmol) in MeCN (10 mL) to afford compound **6** as a yellowish solid (42%). M.P.: 173.2–176.1 °C. ^{1}H NMR (600 MHz, $CDCl_3$): δ 7.81 (d, *J* = 23.4 Hz, 1H), 7.67 (d, *J* = 8.7 Hz, 1H), 7.28 – 7.26 (m, 1H), 6.92 (dd, *J* = 8.8, 2.2 Hz, 1H), 6.56 (s, 1H), 6.46 (s, 1H), 4.81 – 4.67 (m, 2H), 4.28 – 4.13 (m, 4H), 3.82 (d, *J* = 4.8 Hz, 6H), 3.48 (s, 2H), 2.78 (t, *J* = 6.0 Hz, 2H), 2.64 (q, *J* = 5.5 Hz, 2H), 2.50 (t, *J* = 7.2 Hz, 2H), 1.98 – 1.93 (m, 2H), 1.63 – 1.57 (m, 2H). ^{19}F NMR (565 MHz, $CDCl_3$): δ -223.47. ^{13}C NMR (150 MHz, $CDCl_3$): δ 155.54, 147.70, 147.37, 142.62, 139.03, 134.43, 128.95, 126.13, 121.03, 113.81, 111.72, 111.47, 110.33, 109.56, 103.68, 95.03, 82.11 (d, *J* = 170.6 Hz), 68.10, 57.34, 56.00, 51.07, 45.00, 28.66, 27.52, 24.35. HR–MS calcd. for $C_{24}H_{31}FN_3O_3$ $[M + H]^+$ *m*/*z* 428.2344; found *m*/*z* 428.2341.

1-(Benzyloxy)-4-iodobenzene (**42**). To a solution of compound **40** (1,300 mg, 4 mmol) in DMF (20 mL), were added K_2CO_3 (5,545 mg, 25 mmol) and benzyl bromide (5,131 mg, 30 mmol). The mixture was stirred at room temperature for 2 h, filtered and the solvent removed under reduced pressure. The residue was treated with water (100 mL) and extracted with CH_2Cl_2 (5 × 10 mL). The combined extracts were washed with water, dried over anhydrous Na_2SO_4, and concentrated. The

crude product was purified by flash column chromatography on silica gel (hexane = 100%) to yield compound **42** as a white solid (98%). ^{1}H NMR (600 MHz, DMSO-d_6): δ 7.59 (d, *J* = 9.0 Hz, 2H), 7.43 – 7.42 (m, 2H), 7.40 – 7.37 (m, 2H), 7.34 – 7.31 (m, 1H), 6.87 (d, *J* = 9.1 Hz, 2H), 5.09 (d, *J* = 4.3 Hz, 2H). ESI-MS calcd. for $C_{13}H_{12}IO$ $[M + H]^+$ *m*/*z* 310.99; found *m*/*z* 310.97.

1-(Benzyloxy)-3-iodobenzene (**43**). The procedure for the synthesis of **42** was applied to compound **41** (1,300 g, 4 mmol), K_2CO_3 (5,545 mg, 25 mmol) and benzyl bromide (5,131 mg, 30 mmol) in DMF (20 mL) to afford compound **43** as a white solid (98%). ^{1}H NMR (600 MHz, $CDCl_3$): δ 7.44 – 7.37 (m, 4H), 7.37 – 7.32 (m, 2H), 7.31 – 7.29 (m, 1H), 7.00 (td, *J* = 8.1, 2.2 Hz, 1H), 6.97 – 6.91 (m, 1H), 5.03 (s, 2H). ESI-MS calcd. for $C_{13}H_{12}IO$ $[M + H]^+$ *m*/*z* 310.99; found *m*/*z* 310.99.

4-(4-(Benzyloxy)phenyl)but-3-yn-1-ol (**46**). To a solution of compound **42** (1,551 mg, 5 mmol) were added **44** (421 mg, 6 mmol) and TEA (759 mg, 7.5 mmol) in CH_2Cl_2 (20 mL). The mixture was stirred at room temperature for 10 min, followed by addition of $(PPh_3)_2PdCl_2$ (351 mg, 10% mmol) and CuI (72 mg, 7.5% mmol). After stirring at room temperature for 1 h, the mixture was heated to 50 °C and reacted overnight. The mixture was filtered and the solvent removed under reduced pressure. The residue was then treated with water (50 mL) and extracted with CH_2Cl_2 (5 × 10 mL). The combined extracts were washed with water, dried over anhydrous Na_2SO_4, and concentrated. The crude product was purified by flash column chromatography on silica gel (hexane/EtOAc = 4/1) to yield compound **46** as a brownish solid (87%). ^{1}H NMR (600 MHz, $CDCl_3$): δ 7.43 – 7.38 (m, 4H), 7.36 – 7.32 (m, 3H), 6.91 – 6.87 (m, 2H), 5.06 (s, 2H), 3.80 (t, *J* = 6.3 Hz, 2H), 2.68 (t, *J* = 6.2 Hz, 2H), 1.88 (s, 1H). ESI-MS calcd. for $C_{17}H_{17}O_2$ $[M + H]^+$ *m*/*z* 253.12; found *m*/*z* 253.13.

4-(3-(Benzyloxy)phenyl)but-3-yn-1-ol (**47**). The procedure for the synthesis of **46** was applied to compound **43** (1,550 mg, 5 mmol), **44** (420 mg, 6 mmol), TEA (759 mg, 7.5 mmol), $(PPh_3)_2PdCl_2$ (350 mg, 10% mmol) and CuI (75 mg, 7.5% mmol) in CH_2Cl_2 (20 mL) to afford compound **47** as a white solid (95%). ^{1}H NMR (400 MHz, $CDCl_3$): δ 7.47 – 7.37 (m, 5H), 7.21 (t, *J* = 7.8 Hz, 1H), 7.08 – 7.01 (m, 2H), 6.93 (ddd, *J* = 8.4, 2.4, 1.1 Hz, 1H), 5.05 (s, 2H), 3.81 (q, *J* = 5.5, 5.0 Hz, 2H), 2.69 (t, *J* = 6.3 Hz, 2H), 2.02 (s, 1H). ESI-MS calcd. for $C_{17}H_{17}O_2$ $[M + H]^+$ *m*/*z* 253.12; found *m*/*z* 253.15.

5-(4-(Benzyloxy)phenyl)pent-4-yn-1-ol (**48**). The procedure for the synthesis of **46** was applied to compound **42** (1,550 mg, 5 mmol), **45** (430 mg, 6 mmol), TEA (740 mg, 7 mmol), $(PPh_3)_2PdCl_2$

(350 mg, 10% mmol) and CuI (75 mg, 7.5% mmol) in CH_2Cl_2 (20 mL) to afford compound **48** as a yellowish solid (97%). ^{1}H NMR (400 MHz, $CDCl_3$): δ 7.43 – 7.37 (m, 4H), 7.35 – 7.31 (m, 3H), 6.93 – 6.85 (m, 2H), 5.05 (s, 2H), 3.82 (t, *J* = 6.1 Hz, 2H), 2.52 (t, *J* = 6.9 Hz, 2H), 1.91 – 1.80 (m, 2H), 1.60 (s, 1H). ESI-MS calcd. for $C_{18}H_{19}O_2$ $[M + H]^+$ *m*/*z* 267.14; found *m*/*z* 267.16.

5-(3-(Benzyloxy)phenyl)pent-4-yn-1-ol (**49**). The procedure for the synthesis of **46** was applied to compound **43** (1,665 mg, 5 mmol), **45** (435 mg, 6 mmol), TEA (750 mg, 7 mmol), $(PPh_3)_2PdCl_2$ (355 mg, 10% mmol) and CuI (70 mg, 7.5% mmol) in CH_2Cl_2 (20 mL) to afford compound **49** as a yellowish solid (95%). ^{1}H NMR (600 MHz, $CDCl_3$): δ 7.43 (d, *J* = 6.8 Hz, 2H), 7.39 (t, *J* = 7.5 Hz, 2H), 7.36 – 7.31 (m, 1H), 7.22 – 7.17 (m, 1H), 7.05 – 6.99 (m, 2H), 6.91 (ddd, *J* = 8.4, 2.6, 1.0 Hz, 1H), 5.05 (s, 2H), 3.82 (t, *J* = 6.2 Hz, 2H), 2.54 (t, *J* = 7.0 Hz, 2H), 1.90 – 1.83 (m, 2H), 1.63 (s, 1H). ESI-MS calcd. for $C_{18}H_{19}O_2$ $[M + H]^+$ *m*/*z* 267.14; found *m*/*z* 267.17.

1-(Benzyloxy)-4-(4-bromobut-1-yn-1-yl)benzene (**50**). To a solution of compound **46** (1,080 mg, 4.3 mmol) and CBr_4 (1,711 mg, 5.16 mmol) in CH_2Cl_2 (20 mL) in an ice bath was added TPP (1,345 mg, 5.16 mmol) dropwise. The mixture was stirred at room temperature for 12 h, filtered and the solvent removed under reduced pressure. The residue was treated with water (50 mL) and extracted with CH_2Cl_2 (5 × 10 mL). The combined extracts were washed with water, dried over anhydrous Na_2SO_4, and concentrated. The crude product was purified by flash column chromatography on silica gel (hexane/EtOAc = 20/1) to yield compound **50** as a white solid (95%). ^{1}H NMR (600 MHz, $CDCl_3$): δ 7.43 – 7.37 (m, 4H), 7.36 – 7.32 (m, 3H), 6.93 – 6.87 (m, 2H), 5.06 (s, 2H), 3.51 (t, *J* = 7.4 Hz, 2H), 2.96 (t, *J* = 7.4 Hz, 2H). ESI-MS calcd. for $C_{17}H_{16}BrO$ $[M + H]^+$ *m*/*z* 315.04; found *m*/*z* 315.07.

1-(Benzyloxy)-3-(4-bromobut-1-yn-1-yl)benzene (**51**). The procedure for the synthesis of **50** was applied to intermediate **47** (1,150 mg, 4.5 mmol), CBr_4 (1,716 mg, 5.2 mmol) and TPP (1,340 mg, 5.15 mmol) in CH_2Cl_2 (20 mL) to afford compound **51** as a white solid (95%). ^{1}H NMR (400 MHz, $CDCl_3$): δ 7.45 – 7.33 (m, 5H), 7.28 – 7.20 (m, 1H), 7.07 – 7.05 (m, 2H), 6.97 – 6.94 (m, 1H), 5.06 (s, 2H), 3.53 (t, *J* = 7.4 Hz, 2H), 2.98 (t, *J* = 7.3 Hz, 2H). ESI-MS calcd. for $C_{17}H_{16}BrO$ $[M + H]^+$ *m*/*z* 315.04; found *m*/*z* 315.07.

1-(Benzyloxy)-4-(5-bromopent-1-yn-1-yl)benzene (**52**). The procedure for the synthesis of **50** was applied to intermediate **48** (1,165 mg, 4.8 mmol), CBr_4 (1,700 mg, 5 mmol) and TPP (1,330 mg,

5 mmol) in CH_2Cl_2 (20 mL) to afford compound **52** as a white solid (95%). ^{1}H NMR (600 MHz, $CDCl_3$): δ 7.48 (d, *J* = 6.8 Hz, 2H), 7.45 – 7.43 (m, 2H), 7.40 – 7.37 (m, 1H), 7.25 (t, *J* = 7.9 Hz, 1H), 7.10 – 7.08 (m, 2H), 6.98 (ddd, *J* = 8.3, 2.6, 1.0 Hz, 1H), 5.08 (s, 2H), 3.61 (t, *J* = 6.5 Hz, 2H), 2.64 (t, *J* = 6.8 Hz, 2H), 2.17 (q, *J* = 6.7 Hz, 2H). ESI-MS calcd. for $C_{18}H_{18}BrO$ $[M + H]^+$ *m*/*z* 329.05; found *m*/*z* 329.08.

1-(Benzyloxy)-3-(5-bromopent-1-yn-1-yl)benzene (**53**). The procedure for the synthesis of **50** was applied to intermediate **49** (1,160 mg, 4.8 mmol), CBr_4 (1,700 mg, 5 mmol) and TPP (1,330 mg, 5 mmol) in CH_2Cl_2 (20 mL) to afford compound **53** as a white solid (82%). ^{1}H NMR (600 MHz, $CDCl_3$): δ 7.48 (d, *J* = 6.8 Hz, 2H), 7.46 – 7.41 (m, 2H), 7.41 – 7.35 (m, 1H), 7.25 (t, *J* = 7.9 Hz, 1H), 7.12 – 7.06 (m, 2H), 6.97 (ddd, *J* = 8.3, 2.6, 1.0 Hz, 1H), 5.08 (s, 2H), 3.61 (t, *J* = 6.5 Hz, 2H), 2.64 (t, *J* = 6.8 Hz, 2H), 2.16 (q, *J* = 6.7 Hz, 2H). ESI-MS calcd. for $C_{18}H_{18}BrO$ $[M + H]^+$ *m*/*z* 329.05; found *m*/*z* 329.08.

2-(4-(4-(Benzyloxy)phenyl)but-3-yn-1-yl)-6,7-dimethoxy-1,2,3,4-tetrahydroiso-quinoline (**54**). To a solution of intermediate **50** (315 mg, 1 mmol) in anhydrous MeCN (20 mL) were added K_2CO_3 (415 mg, 3 mmol), 6,7-dimethoxy-1,2,3,4-tetrahydroisoquinoline (253 mg, 1.1 mmol) and NaI (37 mg, 0.2 mmol). The mixture was refluxed for 12 h, cooled to room temperature, filtered, and the solvent removed under reduced pressure. The residue was treated with water (20 mL) and extracted with CH_2Cl_2 (3 × 10 mL). The combined extracts were washed with water, dried over anhydrous Na_2SO_4, and concentrated. The crude product was purified by flash column chromatography on silica gel (CH_2Cl_2/MeOH = 40/1) to yield compound **54** as a white solid (60%). ^{1}H NMR (600 MHz, $CDCl_3$): δ 7.43 – 7.37 (m, 4H), 7.35 – 7.31 (m, 3H), 6.90 – 6.88 (m, 2H), 6.60 (s, 1H), 6.52 (s, 1H), 5.06 (s, 2H), 3.84 (s, 3H), 3.83 (s, 3H), 3.67 (s, 2H), 2.86 – 2.81 (m, 6H), 2.71 (t, *J* = 7.7 Hz, 2H). ESI-MS calcd. for $C_{28}H_{30}NO_3$ $[M + H]^+$ *m*/*z* 428.22; found *m*/*z* 428.24.

2-(4-(3-(Benzyloxy)phenyl)but-3-yn-1-yl)-6,7-dimethoxy-1,2,3,4-tetrahydroiso-quinoline (**55**). The procedure for the synthesis of **54** was applied to intermediate **51** (350 mg, 1.2 mmol), K_2CO_3 (400 mg, 2.8 mmol), 6,7-dimethoxy-1,2,3,4-tetrahydroisoquinoline (250 mg, 1 mmol) and NaI (35 mg, 0.2 mmol) in anhydrous MeCN (20 mL) to afford compound **55** as a white solid (42%). ^{1}H NMR (400 MHz, $CDCl_3$): δ 7.43 – 7.33 (m, 5H), 7.20 (t, *J* = 7.9 Hz, 1H), 7.05 (d, *J* = 1.9 Hz, 2H), 6.93 – 6.90

(m, 1H), 6.60 (s, 1H), 6.54 (s, 1H), 5.03 (s, 2H), 3.84 (d, *J* = 3.7 Hz, 6H), 3.66 (s, 2H), 2.88 – 2.80 (m, 6H), 2.73 – 2.69 (m, 2H). ESI-MS calcd. for $C_{28}H_{30}NO_3$ $[M + H]^+$ *m*/*z* 428.22; found *m*/*z* 428.26.

2-(5-(4-(Benzyloxy)phenyl)pent-4-yn-1-yl)-6,7-dimethoxy-1,2,3,4-tetrahydroiso-quinoline (**56**). The procedure for the synthesis of **54** was applied to intermediate **52** (360 mg, 1.3 mmol), K_2CO_3 (450 mg, 3 mmol), 6,7-dimethoxy-1,2,3,4-tetrahydroisoquinoline (300 mg, 1.2 mmol) and NaI (36 mg, 0.2 mmol) in anhydrous MeCN (20 mL) to afford compound **56** as a white solid (49%). ^{1}H NMR (400 MHz, $CDCl_3$): δ 7.43 – 7.33 (m, 7H), 6.89 (d, *J* = 8.8 Hz, 2H), 6.60 (s, 1H), 6.53 (s, 1H), 5.05 (s, 2H), 3.84 (d, *J* = 4.2 Hz, 6H), 3.59 (s, 2H), 2.84 (t, *J* = 5.9 Hz, 2H), 2.74 (t, *J* = 6.6 Hz, 2H), 2.66 (t, *J* = 6.7 Hz, 2H), 2.49 (t, *J* = 7.0 Hz, 2H), 1.90 (q, *J* = 7.2 Hz, 2H). ESI-MS calcd. for $C_{29}H_{32}NO_3$ $[M + H]^+$ *m*/*z* 442.24; found *m*/*z* 442.28.

2-(5-(3-(Benzyloxy)phenyl)pent-4-yn-1-yl)-6,7-dimethoxy-1,2,3,4-tetrahydroiso-quinoline (**57**). The procedure for the synthesis of **54** was applied to intermediate **53** (365 mg, 1.4 mmol), K_2CO_3 (455 mg, 3 mmol), 6,7-dimethoxy-1,2,3,4-tetrahydroisoquinoline (310 mg, 1.2 mmol) and NaI (34 mg, 0.2 mmol) in anhydrous MeCN (20 mL) to afford compound **57** as a white solid (59%). ^{1}H NMR (600 MHz, $CDCl_3$): δ 7.42 (d, *J* = 8.0 Hz, 2H), 7.39 (t, *J* = 7.5 Hz, 2H), 7.36 – 7.29 (m, 1H), 7.22 – 7.16 (m, 1H), 7.05 – 6.98 (m, 2H), 6.90 (ddd, *J* = 8.3, 2.6, 1.1 Hz, 1H), 6.60 (s, 1H), 6.53 (s, 1H), 5.05 (s, 2H), 3.84 (d, *J* = 7.0 Hz, 6H), 3.61 (s, 2H), 2.85 (t, *J* = 6.0 Hz, 2H), 2.76 (t, *J* = 5.9 Hz, 2H), 2.68 (t, *J* = 7.4 Hz, 2H), 2.50 (t, *J* = 7.1 Hz, 2H), 1.91 (q, *J* = 7.2 Hz, 2H). ESI-MS calcd. for $C_{29}H_{32}NO_3$ $[M + H]^+$ *m*/*z* 442.24; found *m*/*z* 442.31.

4-(4-(6,7-Dimethoxy-3,4-dihydroisoquinolin-2(1H)-yl)butyl)phenol (**58**). To a solution of compound **54** (247 mg, 0.58 mmol) in CH_3OH (10 mL) was added 10% Pd/C (13 mg, 20% mmol). The mixture was stirred at 50 °C for 10 h under H_2 atmosphere, cooled to room temperature, filtered, and the solvent removed under reduced pressure. The crude product was re-dissolved in CH_2Cl_2 (2 mL) and purified by flash column chromatography on silica gel (CH_2Cl_2/MeOH = 40/1) to yield compound **58** as a white solid (75%). ^{1}H NMR (600 MHz, $CDCl_3$): δ 6.93 (d, *J* = 8.4 Hz, 2H), 6.62 (d, *J* = 8.4 Hz, 2H), 6.57 (s, 1H), 6.52 (s, 1H), 3.83 (d, *J* = 1.7 Hz, 6H), 3.62 (s, 2H), 2.85 (t, *J* = 5.9 Hz, 2H), 2.79 (t, *J* = 5.8 Hz, 2H), 2.54 (t, *J* = 7.8 Hz, 2H), 2.47 (t, *J* = 7.8 Hz, 2H), 1.67 – 1.56 (m, 4H). ESI-MS calcd. for $C_{21}H_{28}NO_3$ $[M + H]^+$ *m*/*z* 342.21; found *m*/*z* 342.23.

3-(4-(6,7-Dimethoxy-3,4-dihydroisoquinolin-2(1H)-yl)butyl)phenol (**59**). The procedure for the synthesis of **58** was applied to intermediate **55** (250 mg, 0.59 mmol) and 10% Pd/C (13 mg, 20% mmol) in CH_3OH (10 mL) under H_2 atmosphere to afford compound **59** as a white solid (89%). ^1H NMR (600 MHz, $CDCl_3$): δ 7.05 (t, *J* = 7.8 Hz, 1H), 6.65 (d, *J* = 7.8 Hz, 1H), 6.57 (s, 1H), 6.55 – 6.47 (m, 3H), 3.82 (d, *J* = 1.9 Hz, 6H), 3.59 (s, 2H), 2.84 (t, *J* = 5.9 Hz, 2H), 2.77 (t, *J* = 5.9 Hz, 2H), 2.55 (t, *J* = 7.3 Hz, 2H), 2.51 (t, *J* = 6.9 Hz, 2H), 1.66 – 1.58 (m, 4H). ESI-MS calcd. for $C_{21}H_{28}NO_3$ $[M + H]^+$ *m*/*z* 342.21; found *m*/*z* 342.26.

4-(5-(6,7-Dimethoxy-3,4-dihydroisoquinolin-2(1H)-yl)pentyl)phenol (**60**). The procedure for the synthesis of **58** was applied to intermediate **56** (300 mg, 0.65 mmol) and 10% Pd/C (15 mg, 20% mmol) in CH_3OH (10 mL) under H_2 atmosphere to afford compound **60** as a white solid (77%). ^1H NMR (600 MHz, $CDCl_3$): δ 6.92 (d, *J* = 8.4 Hz, 2H), 6.62 (d, *J* = 8.4 Hz, 2H), 6.57 (s, 1H), 6.52 (s, 1H), 3.83 (d, *J* = 1.7 Hz, 6H), 3.62 (s, 2H), 2.85 (t, *J* = 5.9 Hz, 2H), 2.79 (t, *J* = 5.8 Hz, 2H), 2.53 (t, *J* = 7.3 Hz, 2H), 2.47 (t, *J* = 6.9 Hz, 2H), 1.64 (p, *J* = 7.9 Hz, 2H), 1.56 (p, *J* = 7.7 Hz, 2H), 1.34 (p, *J* = 7.6 Hz, 2H). ESI-MS calcd. for $C_{22}H_{30}NO_3$ $[M + H]^+$ *m*/*z* 356.22; found *m*/*z* 356.26.

3-(5-(6,7-Dimethoxy-3,4-dihydroisoquinolin-2(1H)-yl)pentyl)phenol (**61**). The procedure for the synthesis of **58** was applied to intermediate **57** (280 mg, 0.6 mmol) and 10% Pd/C (15 mg, 20% mmol) in CH_3OH (10 mL) under H_2 atmosphere to afford compound **61** as a white solid (80%). ^1H NMR (400 MHz, $CDCl_3$): δ 7.05 (t, *J* = 7.7 Hz, 1H), 6.64 (d, *J* = 7.6 Hz, 1H), 6.57 (s, 1H), 6.54 – 6.50 (m, 3H), 3.82 (s, 6H), 3.62 (s, 2H), 2.87 – 2.84 (m, 2H), 2.80 – 2.77 (m, 2H), 2.53 (t, *J* = 7.3 Hz, 2H), 2.47 (t, *J* = 7.6 Hz, 2H), 1.65 – 1.61 (m, 2H), 1.59 – 1.55 (m, 2H), 1.36 – 1.31 (m, 2H). ESI-MS calcd. for $C_{22}H_{30}NO_3$ $[M + H]^+$ *m*/*z* 356.22; found *m*/*z* 356.28.

2-(4-(4-(2-Fluoroethoxy)phenyl)butyl)-6,7-dimethoxy-1,2,3,4-tetrahydroisoquinoline (**7**). To a solution of intermediate **58** (195 mg, 0.57 mmol) in anhydrous MeCN (10 mL) were added TEA (61 mg, 0.6 mmol), substrate **S5** (262 mg, 1.2 mmol) and KOH (34 mg, 0.6 mmol). The mixture was refluxed at 90 °C for 0.5–1 h, cooled to room temperature, filtered and the solvent removed under reduced pressure. The residue was treated with water (20 mL) and extracted with CH_2Cl_2 (3 × 10 mL). The combined extracts were washed with water, dried over anhydrous Na_2SO_4, and concentrated. The crude product was purified by flash column chromatography on silica gel

(EtOAc/hexane/TEA = 1/4/0.05) to yield compound **7** as a white solid (73%). M.P.: 67.3–68.9 °C. ^{1}H NMR (600 MHz, $CDCl_3$): δ 7.11 (d, *J* = 8.6 Hz, 2H), 6.85 (d, *J* = 8.6 Hz, 2H), 6.58 (s, 1H), 6.51 (s, 1H), 4.79 – 4.77 (m, 1H), 4.71 – 4.69 (m, 1H), 4.22 – 4.21 (m, 1H), 4.18 – 4.16 (m, 1H), 3.83 (d, *J* = 3.9 Hz, 6H), 3.54 (s, 2H), 2.82 (t, *J* = 5.9 Hz, 2H), 2.70 (t, *J* = 5.9 Hz, 2H), 2.60 (t, *J* = 7.1 Hz, 2H), 2.52 (t, *J* = 7.1 Hz, 2H), 1.68 – 1.60 (m, 4H). ^{19}F NMR (565 MHz, $CDCl_3$): δ -223.72. ^{13}C NMR (150 MHz, $CDCl_3$): δ 156.65, 147.64, 147.33, 135.36, 129.46, 114.64, 111.49, 109.63, 82.10 (d, *J* = 170.5 Hz), 67.31 (d, *J* = 20.7 Hz), 58.26, 57.14 – 54.36 (m), 51.13, 34.99, 29.59, 28.65, 26.83. HR–MS calcd. for $C_{23}H_{31}FNO_3$ $[M + H]^+$ *m*/*z* 388.2282; found *m*/*z* 388.2291.

2-(4-(4-(3-Fluoropropoxy)phenyl)butyl)-6,7-dimethoxy-1,2,3,4-tetrahydroisoquinoline (**8**). The procedure for the synthesis of **7** was applied to intermediate **58** (341 mg, 1 mmol), TEA (121 mg, 1.2 mmol), substrate **S6** (464 mg, 2 mmol) and KOH (68 mg, 1.2 mmol) in anhydrous MeCN (20 mL) to afford compound **8** as a white solid (96%). M.P.: 65.0–65.8 °C. ^{1}H NMR (600 MHz, $CDCl_3$): δ 7.09 (d, *J* = 8.5 Hz, 2H), 6.82 (d, *J* = 8.6 Hz, 2H), 6.58 (s, 1H), 6.51 (s, 1H), 4.68 (t, *J* = 5.8 Hz, 1H), 4.60 (t, *J* = 5.8 Hz, 1H), 4.07 (t, *J* = 6.1 Hz, 2H), 3.83 (d, *J* = 4.0 Hz, 6H), 3.54 (s, 2H) 2.82 (t, *J* = 5.9 Hz, 2H), 2.70 (t, *J* = 6.0 Hz, 2H), 2.59 (t, *J* = 7.0 Hz, 2H), 2.52 (t, *J* = 7.0 Hz, 2H), 2.20 – 2.11 (m, 2H), 1.68 – 1.60 (m, 4H). ^{19}F NMR (565 MHz, $CDCl_3$): δ -222.03. ^{13}C NMR (150 MHz, $CDCl_3$): δ 156.97, 147.61, 147.30, 134.90, 129.40, 126.68, 126.29, 114.45, 111.47, 109.60, 80.91 (d, *J* = 164.2 Hz), 63.62 (d, *J* = 5.5 Hz), 58.31, 56.00 (d, *J* = 4.3 Hz), 55.83, 51.15, 35.00, 30.57 (d, *J* = 19.8 Hz), 29.66, 28.69, 26.86. HR–MS calcd. for $C_{24}H_{33}FNO_3$ $[M + H]^+$ *m*/*z* 402.2439; found *m*/*z* 402.2440.

2-(4-(4-(4-Fluorobutoxy)phenyl)butyl)-6,7-dimethoxy-1,2,3,4-tetrahydroisoquinoline (**9**). The procedure for the synthesis of **7** was applied to intermediate **58** (341 mg, 1 mmol), TEA (121 mg, 1.2 mmol), substrate **S7** (492 mg, 2 mmol) and KOH (68 mg, 1.2 mmol) in anhydrous MeCN (20 mL) to afford compound **9** as a white solid (83%). M.P.: 56.3–59.1 °C. ^{1}H NMR (600 MHz, $CDCl_3$): δ 7.09 (d, *J* = 8.2 Hz, 2H), 6.81 (d, *J* = 8.4 Hz, 2H), 6.58 (s, 1H), 6.51 (s, 1H), 4.56 (t, *J* = 5.6 Hz, 1H), 4.48 (t, *J* = 5.6 Hz, 1H), 3.98 (t, *J* = 5.7 Hz, 2H), 3.83 (d, *J* = 3.9 Hz, 6H), 3.54 (s, 2H), 2.81 (t, *J* = 5.9 Hz, 2H), 2.69 (t, *J* = 5.8 Hz, 2H), 2.59 (t, *J* = 7.0 Hz, 2H), 2.51 (t, *J* = 7.0 Hz, 2H), 1.94 – 1.84 (m, 4H), 1.68 – 1.60 (m, 4H). ^{19}F NMR (565 MHz, $CDCl_3$): δ -218.32. ^{13}C NMR (150 MHz, $CDCl_3$): δ 157.12,

147.61, 147.30, 134.72, 129.38, 126.70, 126.30, 114.42, 111.47, 109.61, 83.90 (d, *J* = 164.6 Hz), 67.35, 58.32, 56.00 (d, *J* = 4.3 Hz), 55.84, 51.15, 35.00, 29.67, 28.70, 27.33 (d, *J* = 19.9 Hz), 26.88, 25.39 (d, *J* = 5.1 Hz). HR–MS calcd. for $C_{25}H_{35}FNO_3$ $[M + H]^+$ *m*/*z* 416.2595; found *m*/*z* 416.2599.

2-(4-(4-(2-(2-Fluoroethoxy)ethoxy)phenyl)butyl)-6,7-dimethoxy-1,2,3,4-tetra-hydroisoquinoline (**10**). The procedure for the synthesis of **7** was applied to intermediate **58** (340 mg, 1 mmol), TEA (121 mg, 1.2 mmol), substrate **S8** (524 mg, 2 mmol) and KOH (68 mg, 1.2 mmol) in anhydrous MeCN (20 mL) to afford compound **10** as a white solid (89%). M.P.: 67.3–69.2 °C. ^{1}H NMR (400 MHz, $CDCl_3$): δ 7.09 (d, *J* = 8.5 Hz, 2H), 6.84 (d, *J* = 8.5 Hz, 2H), 6.58 (s, 1H), 6.51 (s, 1H), 4.65 (t, *J* = 5.8 Hz, 1H), 4.53 (t, *J* = 5.8 Hz, 1H), 4.12 (t, *J* = 6.1 Hz, 2H), 3.89 – 3.86 (m, 3H), 3.83 (d, *J* = 3.9 Hz, 6H), 3.79 – 3.77 (m, 1H), 3.55 (s, 2H), 2.82 (t, *J* = 5.9 Hz, 2H), 2.70 (t, *J* = 5.8 Hz, 2H), 2.59 (t, *J* = 6.7 Hz, 2H), 2.52 (t, *J* = 6.7 Hz, 2H), 1.69 – 1.59 (m, 4H). ^{19}F NMR (375 MHz, $CDCl_3$): δ -222.82. ^{13}C NMR (150 MHz, $CDCl_3$): δ 156.92, 147.63, 147.32, 134.96, 129.37, 126.21, 114.60, 111.45, 109.59, 83.26 (d, *J* = 169.0 Hz), 70.67 (d, *J* = 19.6 Hz), 70.11, 67.62, 58.25, 56.00 (d, *J* = 4.9 Hz), 55.75, 51.11, 34.98, 29.61, 28.60, 26.79. HR–MS calcd. for $C_{25}H_{35}FNO_4$ $[M + H]^+$ *m*/*z* 432.2545; found *m*/*z* 432.2543.

2-(4-(4-(2-(2-(2-Fluoroethoxy)ethoxy)ethoxy)phenyl)butyl)-6,7-dimethoxy-1,2,3,4-tetrahydro-isoquinoline (**11**). The procedure for the synthesis of **7** was applied to intermediate **58** (340 mg, 1 mmol), TEA (121 mg, 1.2 mmol), substrate **S9** (612 mg, 2 mmol) and KOH (68 mg, 1.2 mmol) in anhydrous MeCN (20 mL) to afford compound **11** as a white solid (61%). M.P.: 49.7–51.3 °C. ^{1}H NMR (400 MHz, $CDCl_3$): δ 7.07 (d, *J* = 8.6 Hz, 2H), 6.82 (d, *J* = 8.6 Hz, 2H), 6.57 (s, 1H), 6.49 (s, 1H), 4.60 (t, *J* = 5.8 Hz, 1H), 4.48 (t, *J* = 5.8 Hz, 1H), 4.10 (t, *J* = 6.1 Hz, 2H), 3.85 – 3.81 (m, 8H), 3.78 – 3.76 (m, 1H), 3.74 – 3.72 (m, 2H), 3.71 – 3.68 (m, 3H), 3.51 (s, 2H), 2.80 (t, *J* = 5.9 Hz, 2H), 2.67 (t, *J* = 5.8 Hz, 2H), 2.57 (t, *J* = 6.7 Hz, 2H), 2.49 (t, *J* = 6.7 Hz, 2H), 1.68 – 1.55 (m, 4H). ^{19}F NMR (375 MHz, $CDCl_3$): δ -222.74. ^{13}C NMR (150 MHz, $CDCl_3$): δ 156.98, 147.58, 147.28, 134.90, 129.35, 126.75, 126.31, 114.57, 111.46, 109.60, 83.23 (d, *J* = 168.9 Hz), 70.94, 70.54 (d, *J* = 19.6 Hz), 69.97, 67.55, 58.35, 55.99 (d, *J* = 4.7 Hz), 55.86, 51.17, 35.00, 29.64, 28.74, 26.88. HR–MS calcd. for $C_{27}H_{39}FNO_5$ $[M + H]^+$ *m*/*z* 476.2806; found *m*/*z* 476.2804.

2-(4-(3-(2-Fluoroethoxy)phenyl)butyl)-6,7-dimethoxy-1,2,3,4-tetrahydroisoquinoline (**12**).

The procedure for the synthesis of **7** was applied to intermediate **59** (340 mg, 1 mmol), TEA (121 mg, 1.2 mmol), substrate **S5** (612 mg, 2 mmol) and KOH (68 mg, 1.2 mmol) in anhydrous MeCN (20 mL) to afford compound **12** as a white solid (89%). M.P.: 155.2–158.1 °C. ^{1}H NMR (400 MHz, $CDCl_3$): δ 7.19 (t, *J* = 7.8 Hz, 1H), 6.82 – 6.80 (m, 1H), 6.78 – 6.77 (m, 1H), 6.75 – 6.72 (m, 1H), 6.58 (s, 1H), 6.51 (s, 1H), 4.81 – 4.79 (m, 1H), 4.69 – 4.67 (m, 1H), 4.24 – 4.22 (m, 1H), 4.17 – 4.15 (m, 1H), 3.83 (d, *J* = 2.3 Hz, 6H), 3.53 (s, 2H), 2.81 (t, *J* = 5.9 Hz, 2H), 2.70 – 2.67 (m, 2H), 2.65 – 2.61 (m, 2H), 2.53 – 2.49 (m, 2H), 1.71 – 1.60 (m, 4H). ^{19}F NMR (375 MHz, $CDCl_3$): δ -223.64. ^{13}C NMR (100 MHz, $CDCl_3$): δ 158.55, 147.58, 147.27, 144.38, 129.38, 126.75, 126.31, 121.60, 115.12, 111.69, 111.45, 109.59, 82.07 (d, *J* = 170.5 Hz), 67.08 (d, *J* = 20.5 Hz), 58.31, 56.00, 56.98, 55.88, 51.19, 35.92, 29.28, 28.75, 26.94. HR–MS calcd. for $C_{23}H_{31}FNO_3$ $[M + H]^+$ *m*/*z* 388.2282; found *m*/*z* 388.2277.

2-(5-(4-(2-Fluoroethoxy)phenyl)pentyl)-6,7-dimethoxy-1,2,3,4-tetrahydroiso-quinoline (**13**). The procedure for the synthesis of **7** was applied to intermediate **60** (355 mg, 1 mmol), TEA (121 mg, 1.2 mmol), substrate **S5** (612 mg, 2 mmol) and KOH (68 mg, 1.2 mmol) in anhydrous MeCN (20 mL) to afford compound **13** as a white solid (95%). M.P.: 117.1–120.2 °C. ^{1}H NMR (600 MHz, $CDCl_3$): δ 7.10 (d, *J* = 8.6 Hz, 2H), 6.84 (d, *J* = 8.6 Hz, 2H), 6.58 (s, 1H), 6.51 (s, 1H), 4.78 – 4.77 (m, 1H), 4.70 – 4.69 (m, 1H), 4.22 – 4.20 (m, 1H), 4.17 – 4.16 (m, 1H), 3.83 (d, *J* = 4.2 Hz, 6H), 3.55 (s, 2H), 2.82 (t, *J* = 5.9 Hz, 2H), 2.70 (t, *J* = 5.9 Hz, 2H), 2.57 (t, *J* = 5.8 Hz, 2H), 2.49 (t, *J* = 5.6 Hz, 2H), 1.68 – 1.60 (m, 4H), 1.38 (p, *J* = 7.8 Hz, 2H). ^{19}F NMR (565 MHz, $CDCl_3$): δ -223.72. ^{13}C NMR (100 MHz, $CDCl_3$): δ 156.60, 147.59, 147.29, 135.57, 129.43, 126.72, 126.30, 114.59, 111.45, 109.59, 82.11 (d, *J* = 170.5 Hz), 67.28 (d, *J* = 20.6 Hz), 58.42, 56.01, 55.98, 55.89, 51.14, 35.04, 31.70, 28.71, 27.23 (d, *J* = 5.1 Hz). HR–MS calcd. for $C_{24}H_{33}FNO_3$ $[M + H]^+$ *m*/*z* 402.2439; found *m*/*z* 402.2442.

2-(5-(3-(2-Fluoroethoxy)phenyl)pentyl)-6,7-dimethoxy-1,2,3,4-tetrahydroiso-quinoline (**14**). The procedure for the synthesis of **7** was applied to intermediate **61** (355 mg, 1 mmol), TEA (121 mg, 1.2 mmol), substrate **S5** (612 mg, 2 mmol) and KOH (68 mg, 1.2 mmol) in anhydrous MeCN (20 mL) to afford compound **14** as a white solid (96%). M.P.: 154.2–157.0 °C. ^{1}H NMR (600 MHz, $CDCl_3$): δ 7.19 (t, *J* = 7.8 Hz, 1H), 6.81 (d, *J* = 7.5 Hz, 1H), 6.77 (t, *J* = 2.0 Hz, 1H), 6.73 (dd, *J* = 8.2, 1.7 Hz, 1H), 6.58 (s, 1H), 6.52 (s, 1H), 4.78 – 4.76 (m, 1H), 4.70 – 4.69 (m, 1H), 4.22 – 4.20 (m, 1H), 4.17 –

4.16 (m, 1H), 3.83 (d, *J* = 3.3 Hz, 6H), 3.54 (s, 2H), 2.81 (t, *J* = 5.9 Hz, 2H), 2.69 (t, *J* = 5.9 Hz, 2H), 2.61 – 2.59 (m, 2H), 2.50 – 2.47 (m, 2H), 1.69 – 1.60 (m, 4H), 1.40 (p, *J* = 7.8 Hz, 2H). ^{19}F NMR (375 MHz, $CDCl_3$): δ -223.58. ^{13}C NMR (150 MHz, $CDCl_3$): δ 158.55, 147.59, 147.29, 144.60, 129.37, 126.83, 126.36, 121.58, 115.12, 111.61, 111.50, 109.63, 82.07 (d, *J* = 170.5 Hz), 67.08 (d, *J* = 20.7 Hz), 58.44, 56.01, 55.98, 55.93, 51.18, 35.98, 31.36, 28.76, 27.33, 27.23. HR–MS calcd. for $C_{24}H_{33}FNO_3$ $[M + H]^+$ *m*/*z* 402.2439; found *m*/*z* 402.2441.

1-(2-(Benzyloxy)ethyl)-3-(4-(6,7-dimethoxy-3,4-dihydroisoquinolin-2(1H)-yl)butyl)-1,3-dihyd-ro-2H-benzo[d]imidazol-2-one (**62**). The procedure for the synthesis of **17** was applied to intermediate **19** (250 mg, 1 mmol), K_2CO_3 (256 mg, 2 mmol), TBAI (40 mg, 20% mmol) and ((2-bromoethoxy)methyl)benzene (323 mg, 1.5 mmol) in DMF (10 mL) to afford compound **62** as a yellowish oil (98%). ^{1}H NMR (400 MHz, $CDCl_3$): δ 7.29 – 7.27 (m, 2H), 7.23 – 7.20 (m, 3H), 7.13 – 7.10 (m, 1H), 7.06 – 7.04 (m, 2H), 7.01 – 6.99 (m, 1H), 6.57 (s, 1H), 6.49 (s, 1H), 4.50 (s, 2H), 4.12 – 4.09 (m, 2H), 3.92 (t, *J* = 7.0 Hz, 2H), 3.83 (d, *J* = 2.8 Hz, 6H), 3.77 (t, *J* = 4.0 Hz, 2H), 3.54 (s, 2H), 2.80 (d, *J* = 5.8 Hz, 2H), 2.69 (t, *J* = 5.7 Hz, 2H), 2.55 (t, *J* = 7.2 Hz, 2H), 1.88 – 1.80 (m, 2H), 1.71 – 1.65 (m, 2H). ESI–MS calcd. for $C_{31}H_{38}N_3O_4$ $[M + H]^+$ *m*/*z* 516.29; found *m*/*z* 516.30.

1-(4-(6,7-Dimethoxy-3,4-dihydroisoquinolin-2(1H)-yl)butyl)-3-(2-hydroxyethyl)-1,3-dihydro-2H-benzo[d]imidazol-2-one (**63**). To a solution of intermediate **62** (516 mg, 1 mmol) in MeOH (10 mL) were added 10% Pd/C (30 mg, 20% mmol) and H_2. The mixture was stirred at 50 °C for 10 h, cooled, filtered, and the solvent removed under reduced pressure to afford compound **63** as a white solid (98%). ^{1}H NMR (400 MHz, $CDCl_3$): δ 7.10 – 7.02 (m, 4H), 6.58 (s, 1H), 6.50 (s, 1H), 4.06 – 4.03 (m, 2H), 3.97 – 3.93 (m, 4H), 3.83 (d, *J* = 2.8 Hz, 6H), 3.67 (s, 2H), 2.86 (s, 4H), 2.67 (s, 2H), 1.90 – 1.82 (m, 2H), 1.74 (d, *J* = 8.0 Hz, 2H). ESI–MS calcd. for $C_{24}H_{32}N_3O_4$ $[M + H]^+$ *m*/*z* 426.24; found *m*/*z* 426.25.

2-(3-(4-(6,7-Dimethoxy-3,4-dihydroisoquinolin-2(1H)-yl)butyl)-2-oxo-2,3-dihydro-1H-benzo[d] imidazole-1-yl)ethyl 4-methylbenzenesulfonate (**64**). To a solution of intermediate **63** (148 mg, 0.35 mmol) in CH_2Cl_2 (10 mL), were added TEA (101 mg, 1 mmol) and DMAP (9 mg, 20% mmol). The mixture was stirred at 0 °C and a solution of *p*-toluenesulfonyl chloride (134 mg, 0.7 mmol) in dry CH_2Cl_2 (20 mL) added dropwise. The mixture was then stirred at room temperature for

12 h, treated with water (20 mL) and extracted with CH_2Cl_2 (3 × 10 mL). The combined extracts were washed with water, dried over anhydrous Na_2SO_4, and concentrated. The crude product was purified by silica gel column chromatography (EtOAc/hexane/TEA/MeOH = 20/10/1/1) to yield precursor **64** as a white solid (78%). M.P.: 67.4–69.7 °C. ^{1}H NMR (400 MHz, $CDCl_3$): δ 7.57 (d, *J* = 8.3 Hz, 2H), 7.18 (d, *J* = 8.4 Hz, 2H), 7.07 – 7.02 (m, 3H), 6.97 – 6.95 (m, 1H), 6.57 (s, 1H), 6.49 (s, 1H), 4.31 (t, *J* = 5.3 Hz, 2H), 4.12 (t, *J* = 5.3 Hz, 2H), 3.82 (d, *J* = 5.7 Hz, 8H), 3.55 (s, 2H), 2.80 (d, *J* = 6.0 Hz, 2H), 2.70 (s, 2H), 2.54 (d, *J* = 7.9 Hz, 2H), 2.38 (s, 3H), 1.80 (q, *J* = 7.3 Hz, 2H), 1.66 (q, *J* = 7.8 Hz, 2H). ^{13}C NMR (100 MHz, $CDCl_3$): δ 153.85, 147.59, 147.27, 144.85, 132.44, 129.79, 129.36, 129.26, 127.81, 126.15, 121.54, 121.48, 111.38, 109.52, 108.19, 107.79, 77.35, 67.79, 57.58, 56.00, 55.98, 55.73, 51.07, 40.95, 40.44, 31.67, 28.66, 26.27, 24.33, 22.74, 21.74, 14.22. HR–MS calcd. for $C_{31}H_{38}N_3O_6S$ $[M + H]^+$ *m*/*z* 580.2476; found *m*/*z* 580.2471.

2-((1-(4-(5,6-Dimethoxyisoindolin-2-yl)butyl)-1H-benzo[d]imidazol-5-yl)oxy)eth-yl 4-methyl-benzenesulfonate (**65**). To a solution of intermediate **36** (94 mg, 0.26 mmol) in MeCN (10 mL), were added KOH (28 mg, 0.5 mmol), 1,2-bis(4-methylbenzenesulfonyloxy)ethane (186 mg, 0.5 mmol) and TEA (27 mg, 0.26 mmol). The mixture was stirred at 90 °C for 1 h, cooled, filtered, and the solvent removed under reduced pressure. The residue was treated with water (20 mL) and extracted with CH_2Cl_2 (3 × 10 mL). The combined extracts were washed with water, dried over anhydrous Na_2SO_4, and concentrated. The crude product was purified by silica gel column chromatography (EtOAc/hexane/TEA/MeOH = 25/5/5/1) to yield precursor **65** as an off-white solid (53%). M.P.: 108.7–111.4 °C. ^{1}H NMR (600 MHz, $CDCl_3$): δ 7.81 – 7.77 (m, 3H), 7.62 (dd, *J* = 8.8, 1.5 Hz, 1H), 7.30 (dd, *J* = 8.3, 1.5 Hz, 2H), 6.82 (t, *J* = 2.0 Hz, 1H), 6.75 (dt, *J* = 8.8, 2.0 Hz, 1H), 6.70 (s, 2H), 4.35 – 4.33 (m, 2H), 4.17 – 4.14 (m, 4H), 3.88 (s, 4H), 3.84 (s, 6H), 2.77 – 2.75 (m, 2H), 2.42 (s, 3H), 2.01 – 1.92 (m, 2H), 1.66 – 1.58 (m, 2H). ^{13}C NMR (150 MHz, $CDCl_3$): δ 155.16, 148.70, 145.05, 142.59, 138.98, 134.37, 133.00, 131.02, 129.95, 128.80, 125.84, 120.98, 111.97, 105.96, 94.92, 68.33, 66.56, 59.20, 56.23, 55.22, 44.90, 27.46, 25.81, 21.71. HR–MS calcd. for $C_{30}H_{36}N_3O_6S$ $[M + H]^+$ *m*/*z* 566.2319; found *m*/*z* 566.2321.

***In Vitro* Competition Studies.** All the procedures for radioligand competition studies were performed by the Psychoactive Drug Screening Program (PDSP) of the National Institute of Mental Health (NIMH) and Helmholtz-Zentrum Dresden-Rossendorf (HZDR). Detailed procedures are given in the Supporting Information.

Molecular Docking. According to the methods in the literature[4], the Schrödinger software was used to perform molecular docking calculations on the σ_2 receptors for new compounds with suitable affinity. The structures of complexes σ_2–CM398, σ_2–**1**, σ_2–**2**, σ_2–**3**, σ_2–**4**, σ_2–**7** and σ_2–**12** (Figure 2, S1 and S2) were obtained, respectively. First, the LigPrep program was used to minimize the energy of ligands, set the charge, add polar and nonpolar hydrogens, generate possible ionization states, and define rotatable bonds. The crystal structure of the σ_2 receptor (PDB code: 7MFI) was downloaded from the Protein Data Bank website (www.rcsb.org**),** and the protein was hydrogenated (protonated against basic N atoms) using the Protein Preparation Wizard program to remove the solvent and specify bond levels. The generated receptor mesh file and ligand structure were then docked using the Glide module. The obtained docking results were opened with Pymol for preview, analysis, and graphing.

Synthesis of Radioligands and Determination of Lipophilicity and Stability. Radioligands [^{18}F]**1** and [^{18}F]**4** were prepared with a home-made synthesis module (PET-MF-2 V-IT-I) following the procedures reported previously[37, 55], as illustrated in Scheme 5. Determination of lipophilicity (Log$D_{7.4}$ values) and *in vitro* stability of the radioligands in saline solution (about 7% ethanol) also followed the procedures reported previously[37]. Detailed procedures are provided in the Supporting Information.

Biological evaluation. *Ex vivo* biodistribution studies followed the procedures reported previously[37, 55]. *In vivo* dynamic micro-PET/CT imaging of [^{18}F]**1** in normal rats was performed using a microPET/CT scanner (Inveon PET/CT, Siemens, Germany). The static imaging in nude mice

bearing U87MG glioma xenografts was performed using a Super Nova PET/CT scanner (PINGSHENG Healthcare Inc., China) equipped with a computer-controlled bed (one-bed position). Detailed procedures are provided in the Supporting Information.

ASSOCIATED CONTENT

Supporting information

The Supporting Information is available free of charge at http://pubs.acs.org.

The 2D and 3D diagram of receptor-ligand binding for CM398 (Figure S1); The 2D diagram of receptor-ligand binding (Figure S2); Calibration curves for molar activity determination (Figure S3); HPLC co-elution profiles (Figure S4); Stability analysis of radioligands in saline (Figure S5); Binding affinities of CM398 and novel σ_2 receptor ligands **1**–**14** as measured by PDSP (Table S1); Blocking effect of CM398 on the biodistribution of [^{18}F]**1** in male KM mice (Table S2); Biodistribution of [^{18}F]**4** (Table S3) and blocking effect of CM398 on the biodistribution of [^{18}F]**4** in male ICR mice (Table S4); Effect of P-gp on brain uptake in mice (Table S5); Micro-PET/CT imaging and blocking studies in rats (Figure S6); Time–activity curves (TACs) of [^{18}F]**1** in the bone from micro-PET/CT imaging and blocking studies (Figure S7); Micro-PET/CT imaging and blocking studies in mice bearing U87MG glioma xenografts (Table S6 and Figure S8); HPLC purity tests (Table S7); Structures and NMR spectra, HRMS results, and HPLC profiles of target compounds (PDF).

Molecular docking of ligands CM398, **1**–**4**, **7** and **12** with 7MFI (ZIP).

Molecular formula strings of the target compounds (CSV).

AUTHOR INFORMATION

CORRESPONDING AUTHORS

Hongmei Jia − *Key Laboratory of Radiopharmaceuticals (Beijing Normal University), Ministry of Education, College of Chemistry, Beijing Normal University, Beijing 100875, China;* Email: hmjia@bnu.edu.cn

Yiyun Huang − *Yale PET Center, Department of Radiology and Biomedical Imaging, Yale University School of Medicine, New Haven, CT 06520-8048, USA;* Email: henry.huang@yale.edu

Jinming Zhang − *Nuclear Medicine Department, The First Medical Center of Chinese PLA General Hospital, Beijing 100853, China;* Email: zhangjm301@163.com

AUTHORS

Tao Wang − *Key Laboratory of Radiopharmaceuticals (Beijing Normal University), Ministry of Education, College of Chemistry, Beijing Normal University, Beijing 100875, China;*

Department of Nuclear Medicine, Xinqiao Hospital, Army Medical University, Chongqing 400037, China;

Jingqi Wang − *Key Laboratory of Radiopharmaceuticals (Beijing Normal University), Ministry of Education, College of Chemistry, Beijing Normal University, Beijing 100875, China;*

Leyuan Chen − *Institute of Radiation Medicine, Peking Union Medical College & Chinese Academy of Medical Sciences, Tianjin 300192, China;*

Xiaojun Zhang − *Nuclear Medicine Department, The First Medical Center of Chinese PLA General Hospital, Beijing 100853, China;*

Tiantian Mou − *Department of Nuclear Medicine, Beijing Anzhen Hospital, Capital Medical University, Beijing 100029, China;*

Xiaodan An − *Key Laboratory of Radiopharmaceuticals (Beijing Normal University), Ministry of Education, College of Chemistry, Beijing Normal University, Beijing 100875, China;*

Xiaoli Zhang − *Department of Nuclear Medicine, Beijing Anzhen Hospital, Capital Medical University, Beijing 100029, China;*

Winnie Deuther-Conrad – *Department of Neuroradiopharmaceuticals, Institute of Radiopharmaceutical Cancer Research, Helmholtz-Zentrum Dresden-Rossendorf (HZDR), 04318 Leipzig, Germany.*

AUTHOR CONTRIBUTIONS

[#] Tao Wang and Jingqi Wang contributed equally to this work. Hongmei Jia, Yiyun Huang and Jinming Zhang conceived and designed the study. Tao Wang and Jingqi Wang performed chemical synthesis of compounds. Yiyun Huang and Winnie Deuther-Conrad were responsible for the *in vitro*

radioligand competition binding studies. Leyuan Chen performed the molecular docking experiment. Tao Wang, Jingqi Wang, Xiaojun Zhang, Tiantian Mou, Xiaoli Zhang, Xiaodan An and Jinming Zhang performed the radiochemistry and biological evaluations. Tao Wang, Yiyun Huang, Winnie Deuther-Conrad and Hongmei Jia analyzed the data. Tao Wang, Yiyun Huang and Hongmei Jia wrote the manuscript. All the authors contributed to this manuscript and approved the final version.

NOTES

The authors have no conflicts of interest to declare.

ACKNOWLEDGMENTS

The authors would like to thank Tina Spalholz, HZDR, for her assistance with the radioligand binding experiments. This work was supported by the National Natural Science Foundation of China (grant numbers 22276016 and 21876013).

ABBREVIATIONS

% ID/g, percentage of injected dose per gram; CBr_4, *tetra*-bromomethane; CDI, 1,1′-carbonyldiimidazole; CRC, colorectal cancer; CT, computed tomography; DHP, 3,4-dihydro-2*H*-pyran; HCC, hepatocellular carcinoma; LDLR, low-density lipoprotein receptor; MAC30, meningioma-associated protein; NIMH, National Institute of Mental Health; PGRMC1, progesterone receptor membrane component 1; PDSP, Psychoactive Drug Screening Program; RCP, radiochemical purity; RCY, radiochemical yield; σ, sigma; SUV, standard uptake value; SQCLC, squamous cell carcinoma of lung; SD, Sprague−Dawley; TAC, time–activity curve; TMEM97, transmembrane protein 97; TEA, triethylamine; TBAI, tetrabutylammonium iodide; TsCl, *p*-touenesulfonyl choride.

REFERENCES

(1) Quirion, R.; Bowen, W. D.; Itzhak, Y.; Junien, J. L.; Musacchio, J. M.; Rothman, R. B.; Su, T. P.; Tam, S. W.; Taylor, D. P. A proposal for the classification of sigma binding sites. *Trends Pharmacol Sci* **1992**, *13* (3), 85-86.

(2) Alon, A.; Schmidt, H. R.; Wood, M. D.; Sahn, J. J.; Martin, S. F.; Kruse, A. C. Identification of the gene that codes for the σ_2 receptor. *Proc Natl Acad Sci U S A* **2017**, *114* (27), 7160-7165.
(3) Bartz, F.; Kern, L.; Erz, D.; Zhu, M.; Gilbert, D.; Meinhof, T.; Wirkner, U.; Erfle, H.; Muckenthaler, M.; Pepperkok, R.; et al. Identification of cholesterol-regulating genes by targeted RNAi screening. *Cell Metab* **2009**, *10* (1), 63-75.
(4) Alon, A.; Lyu, J.; Braz, J. M.; Tummino, T. A.; Craik, V.; O'Meara, M. J.; Webb, C. M.; Radchenko, D. S.; Moroz, Y. S.; Huang, X. P.; et al. Structures of the σ_2 receptor enable docking for bioactive ligand discovery. *Nature* **2021**, *600* (7890), 759-764.
(5) Yang, K.; Zeng, C.; Wang, C.; Sun, M.; Yin, D.; Sun, T. Sigma-2 receptor-A potential target for cancer/Alzheimer's disease treatment via its regulation of cholesterol homeostasis. *Molecules* **2020**, *25* (22), 5439.
(6) Mach, R. H.; Zeng, C.; Hawkins, W. G. The σ_2 receptor: a novel protein for the imaging and treatment of cancer. *J Med Chem* **2013**, *56* (18), 7137-7160.
(7) Zeng, C.; Riad, A.; Mach, R. H. The biological function of sigma-2 receptor/TMEM97 and its utility in PET imaging studies in cancer. *Cancers (Basel)* **2020**, *12* (7), 1877.
(8) Izzo, N. J.; Yuede, C. M.; LaBarbera, K. M.; Limegrover, C. S.; Rehak, C.; Yurko, R.; Waybright, L.; Look, G.; Rishton, G.; Safferstein, H.; et al. Preclinical and clinical biomarker studies of CT1812: A novel approach to Alzheimer's disease modification. *Alzheimers Dement* **2021**, *17* (8), 1365-1382.
(9) Grundman, M.; Morgan, R.; Lickliter, J. D.; Schneider, L. S.; DeKosky, S.; Izzo, N. J.; Guttendorf, R.; Higgin, M.; Pribyl, J.; Mozzoni, K.; et al. A phase 1 clinical trial of the sigma-2 receptor complex allosteric antagonist CT1812, a novel therapeutic candidate for Alzheimer's disease. *Alzheimers Dement (N Y)* **2019**, *5*, 20-26.
(10) Limegrover, C. S.; Yurko, R.; Izzo, N. J.; LaBarbera, K. M.; Rehak, C.; Look, G.; Rishton, G.; Safferstein, H.; Catalano, S. M. Sigma-2 receptor antagonists rescue neuronal dysfunction induced by Parkinson's patient brain-derived α-synuclein. *J Neurosci Res* **2021**, *99* (4), 1161-1176.
(11) Davidson, M.; Saoud, J.; Staner, C.; Noel, N.; Luthringer, E.; Werner, S.; Reilly, J.; Schaffhauser, J. Y.; Rabinowitz, J.; Weiser, M.; et al. Efficacy and safety of MIN-101: A 12-week randomized, double-blind, placebo-controlled trial of a new drug in development for the treatment of negative symptoms in schizophrenia. *Am J Psychiatry* **2017**, *174* (12), 1195-1202.
(12) Sahn, J. J.; Mejia, G. L.; Ray, P. R.; Martin, S. F.; Price, T. J. Sigma-2 receptor/Tmem97 agonists produce long lasting antineuropathic pain effects in mice. *ACS Chem Neurosci* **2017**, *8* (8), 1801-1811.
(13) Nuwayhid, S. J.; Werling, L. L. Sigma$_2$ (σ_2) receptors as a target for cocaine action in the rat striatum. *Eur J Pharmacol* **2006**, *535* (1-3), 98-103.
(14) Sánchez, C.; Papp, M. The selective sigma$_2$ ligand Lu 28-179 has an antidepressant-like profile in the rat chronic mild stress model of depression. *Behav Pharmacol* **2000**, *11* (2), 117-124.
(15) Rasheed, A.; Zaheer, A. B.; Munawwar, A.; Sarfraz, Z.; Sarfraz, A.; Robles-Velasco, K.; Cherrez-Ojeda, I. The allosteric antagonist of the sigma-2 receptors-elayta (CT1812) as a therapeutic candidate for mild to moderate Alzheimer's disease: A scoping systematic review. *Life (Basel)* **2022**, *13* (1), 1.
(16) Mach, R. H.; Smith, C. R.; al-Nabulsi, I.; Whirrett, B. R.; Childers, S. R.; Wheeler, K. T. Sigma-2 receptors as potential biomarkers of proliferation in breast cancer. *Cancer Res* **1997**, *57* (1), 156-161.
(17) Al-Nabulsi, I.; Mach, R. H.; Wang, L. M.; Wallen, C. A.; Keng, P. C.; Sten, K.; Childers, S. R.; Wheeler, K. T. Effect of ploidy, recruitment, environmental factors, and tamoxifen treatment on the expression of sigma-2 receptors in proliferating and quiescent tumour cells. *Br J Cancer* **1999**, *81* (6), 925-933.
(18) Wheeler, K. T.; Wang, L. M.; Wallen, C. A.; Childers, S. R.; Cline, J. M.; Keng, P. C.; Mach, R. H. Sigma-2 receptors as a biomarker of proliferation in solid tumours. *Br J Cancer* **2000**, *82* (6), 1223-1232.
(19) Dehdashti, F.; Laforest, R.; Gao, F.; Shoghi, K. I.; Aft, R. L.; Nussenbaum, B.; Kreisel, F. H.; Bartlett, N. L.;

Cashen, A.; Wagner-Johnston, N.; et al. Assessment of cellular proliferation in tumors by PET using ^{18}F-ISO-1. *J Nucl Med* **2013**, *54* (3), 350-357.
(20) McDonald, E. S.; Doot, R. K.; Young, A. J.; Schubert, E. K.; Tchou, J.; Pryma, D. A.; Farwell, M. D.; Nayak, A.; Ziober, A.; Feldman, M. D.; et al. Breast cancer ^{18}F-ISO-1 uptake as a marker of proliferation status. *J Nucl Med* **2020**, *61* (5), 665-670.
(21) Riad, A.; Zeng, C.; Weng, C. C.; Winters, H.; Xu, K.; Makvandi, M.; Metz, T.; Carlin, S.; Mach, R. H. Sigma-2 receptor/TMEM97 and PGRMC-1 increase the rate of internalization of LDL by LDL receptor through the formation of a ternary complex. *Sci Rep* **2018**, *8* (1), 16845.
(22) Qiu, G.; Sun, W.; Zou, Y.; Cai, Z.; Wang, P.; Lin, X.; Huang, J.; Jiang, L.; Ding, X.; Hu, G. RNA interference against TMEM97 inhibits cell proliferation, migration, and invasion in glioma cells. *Tumour Biol* **2015**, *36* (10), 8231-8238.
(23) Ding, H.; Gui, X. H.; Lin, X. B.; Chen, R. H.; Cai, H. R.; Fen, Y.; Sheng, Y. L. Prognostic value of MAC30 expression in human pure squamous cell carcinomas of the lung. *Asian Pac J Cancer Prev* **2016**, *17* (5), 2705-2710.
(24) Wu, X.; Zhang, Y.; Guo, J.; Yan, X.; Shen, L.; Zhou, J.; Zhao, J.; Zhuang, M.; Cao, Z. MAC30 knockdown inhibits proliferation and enhance apoptosis of gastric cancer by suppressing Wnt/β-cateninsignaling pathway. *Gastroenterol Res Pract* **2020**, *2020* (2020), 6358685.
(25) Mao, D.; Zhang, X.; Wang, Z.; Xu, G.; Zhang, Y. TMEM97 is transcriptionally activated by YY1 and promotes colorectal cancer progression via the GSK-3β/β-catenin signaling pathway. *Hum Cell* **2022**, *35* (5), 1535-1546.
(26) Zhang, P.; Tian, Q.; Gao, H.; Zhao, A.; Shao, Y.; Yang, J. Inhibition of MAC30 exerts antitumor effects in nasopharyngeal carcinoma via affecting the Akt/GSK-3β/β-catenin pathway. *J Biochem Mol Toxicol* **2022**, *36* (7), e23061.
(27) Zhang, Y.; Li, H.; Wang, J.; Geng, X.; Hai, J. Meningioma-associated protein 30 accelerates the proliferation and invasion of hepatocellular carcinoma by modulating Wnt/GSK-3β/β-catenin signaling. *J Bioenerg Biomembr* **2021**, *53* (1), 73-83.
(28) Zhu, H.; Su, Z.; Ning, J.; Zhou, L.; Tan, L.; Sayed, S.; Song, J.; Wang, Z.; Li, H.; Sun, Q.; et al. Transmembrane protein 97 exhibits oncogenic properties via enhancing LRP6-mediated Wnt signaling in breast cancer. *Cell Death Dis* **2021**, *12* (10), 912.
(29) Roy, J.; Kyani, A.; Hanafi, M.; Xu, Y.; Takyi-Williams, J.; Sun, D.; Osman, E. E. A.; Neamati, N. Design and synthesis of orally active quinolyl pyrazinamides as sigma 2 receptor ligands for the treatment of pancreatic cancer. *J Med Chem* **2023**, *66* (3), 1990-2019.
(30) Shaghaghi, Z.; Alvandi, M.; Ghanbarimasir, Z.; Farzipour, S.; Emami, S. Current development of sigma-2 receptor radioligands as potential tumor imaging agents. *Bioorg Chem* **2021**, *115*, 105163.
(31) Zeng, C.; McDonald, E. S.; Mach, R. H. Molecular probes for imaging the sigma-2 receptor: In vitro and in vivo imaging studies. *Handb Exp Pharmacol* **2017**, *244*, 309-330.
(32) Xie, F.; Kniess, T.; Neuber, C.; Deuther-Conrad, W.; Mamat, C.; Lieberman, B. P.; Liu, B.; Mach, R. H.; Brust, P.; Steinbach, J.; et al. Novel indole-based sigma-2 receptor ligands: synthesis, structure–affinity relationship and antiproliferative activity. *MedChemComm* **2015**, *6* (6), 1093-1103.
(33) Tu, Z.; Xu, J.; Jones, L. A.; Li, S.; Dumstorff, C.; Vangveravong, S.; Chen, D. L.; Wheeler, K. T.; Welch, M. J.; Mach, R. H. Fluorine-18-labeled benzamide analogues for imaging the σ_2 receptor status of solid tumors with positron emission tomography. *J Med Chem* **2007**, *50* (14), 3194-3204.
(34) Lee, I.; Lieberman, B. P.; Li, S.; Hou, C.; Makvandi, M.; Mach, R. H. Comparative evaluation of 4 and 6-carbon spacer conformationally flexible tetrahydroisoquinolinyl benzamide analogues for imaging the sigma-2 receptor status of solid tumors. *Nucl Med Biol* **2016**, *43* (11), 721-731.

(35) Li, D.; Chen, Y.; Wang, X.; Deuther-Conrad, W.; Chen, X.; Jia, B.; Dong, C.; Steinbach, J.; Brust, P.; Liu, B.; et al. ^{99m}Tc-cyclopentadienyl tricarbonyl chelate-labeled compounds as selective sigma-2 receptor ligands for tumor imaging. *J Med Chem* **2016**, *59* (3), 934-946.
(36) Wang, L.; Ye, J.; He, Y.; Deuther-Conrad, W.; Zhang, J.; Zhang, X.; Cui, M.; Steinbach, J.; Huang, Y.; Brust, P.; et al. ^{18}F-Labeled indole-based analogs as highly selective radioligands for imaging sigma-2 receptors in the brain. *Bioorg Med Chem* **2017**, *25* (14), 3792-3802.
(37) Zhang, Y.; Wang, T.; Zhang, X.; Deuther-Conrad, W.; Fu, H.; Cui, M.; Zhang, J.; Brust, P.; Huang, Y.; Jia, H. Discovery and development of brain-penetrant ^{18}F-labeled radioligands for neuroimaging of the sigma-2 receptors. *Acta Pharm Sin B* **2022**, *12* (3), 1406-1415.
(38) Alluri, S. R.; Zheng, M.; Holden, D.; Zhang, Y.; Li, S.; Felchner, Z.; Zhang, L.; Ropchan, J.; Carson, R.; Jia, H.; et al. Quantitative evaluation of a novel brain-penetrant sigma-2 receptor radioligand in non-human primates. *J Nucl Med* **2022**, *63* (supplement 2), 2845.
(39) Intagliata, S.; Sharma, A.; King, T. I.; Mesangeau, C.; Seminerio, M.; Chin, F. T.; Wilson, L. L.; Matsumoto, R. R.; McLaughlin, J. P.; Avery, B. A.; et al. Discovery of a highly selective sigma-2 receptor ligand, 1-(4-(6,7-Dimethoxy-3,4-dihydroisoquinolin-2(1*H*)-yl)butyl)-3-methyl-1*H*-benzo[*d*]imidazol-2(3*H*)-one (CM398), with drug-like properties and antinociceptive effects in vivo. *AAPS J* **2020**, *22* (5), 94.
(40) Wilson, L. L.; Alleyne, A. R.; Eans, S. O.; Cirino, T. J.; Stacy, H. M.; Mottinelli, M.; Intagliata, S.; McCurdy, C. R.; McLaughlin, J. P. Characterization of CM-398, a novel selective sigma-2 receptor ligand, as a potential therapeutic for neuropathic pain. *Molecules* **2022**, *27* (11), 3617.
(41) Wang, X.; Li, Y.; Deuther-Conrad, W.; Xie, F.; Chen, X.; Cui, M. C.; Zhang, X. J.; Zhang, J. M.; Steinbach, J.; Brust, P.; et al. Synthesis and biological evaluation of ^{18}F labeled fluoro-oligo-ethoxylated 4-benzylpiperazine derivatives for sigma-1 receptor imaging. *Bioorg Med Chem* **2013**, *21* (1), 215-222.
(42) Xu, K.; Hsieh, C. J.; Lee, J. Y.; Riad, A.; Izzo, N. J.; Look, G.; Catalano, S.; Mach, R. H. Exploration of diazaspiro cores as piperazine bioisosteres in the development of σ_2 receptor ligands. *Int J Mol Sci* **2022**, *23* (15), 8259.
(43) Kayed, H.; Kleeff, J.; Ding, J.; Hammer, J.; Giese, T.; Zentgraf, H.; Büchler, M. W.; Friess, H. Expression analysis of MAC30 in human pancreatic cancer and tumors of the gastrointestinal tract. *Histol Histopathol* **2004**, *19* (4), 1021-1031.
(44) Demeule, M.; Régina, A.; Jodoin, J.; Laplante, A.; Dagenais, C.; Berthelet, F.; Moghrabi, A.; Béliveau, R. Drug transport to the brain: key roles for the efflux pump P-glycoprotein in the blood-brain barrier. *Vascul Pharmacol* **2002**, *38* (6), 339-348.
(45) Henson, J. W.; Cordon-Cardo, C.; Posner, J. B. P-glycoprotein expression in brain tumors. *J Neurooncol* **1992**, *14* (1), 37-43.
(46) Hendrikse, N. H.; de Vries, E. G.; Eriks-Fluks, L.; van der Graaf, W. T.; Hospers, G. A.; Willemsen, A. T.; Vaalburg, W.; Franssen, E. J. A new *in vivo* method to study P-glycoprotein transport in tumors and the blood-brain barrier. *Cancer Res* **1999**, *59* (10), 2411-2416.
(47) Demeule, M.; Shedid, D.; Beaulieu, E.; Del Maestro, R. F.; Moghrabi, A.; Ghosn, P. B.; Moumdjian, R.; Berthelet, F.; Béliveau, R. Expression of multidrug-resistance P-glycoprotein (MDR1) in human brain tumors. *Int J Cancer* **2001**, *93* (1), 62-66.
(48) Blanckaert, P.; Burvenich, I.; Staelens, S.; De Bruyne, S.; Moerman, L.; Wyffels, L.; De Vos, F. Effect of cyclosporin A administration on the biodistribution and multipinhole μSPECT imaging of [^{123}I]R91150 in rodent brain. *Eur J Nucl Med Mol Imaging* **2009**, *36* (3), 446-453.
(49) Shao, X.; Carpenter, G. M.; Desmond, T. J.; Sherman, P.; Quesada, C. A.; Fawaz, M.; Brooks, A. F.; Kilbourn, M. R.; Albin, R. L.; Frey, K. A.; et al. Evaluation of [^{11}C]*N*-methyl lansoprazole as a radiopharmaceutical for PET imaging of tau neurofibrillary tangles. *ACS Med Chem Lett* **2012**, *3* (11), 936-941.

(50) Liow, J. S.; Lu, S.; McCarron, J. A.; Hong, J.; Musachio, J. L.; Pike, V. W.; Innis, R. B.; Zoghbi, S. S. Effect of a P-glycoprotein inhibitor, Cyclosporin A, on the disposition in rodent brain and blood of the 5-HT_{1A} receptor radioligand, [^{11}C](*R*)-(-)-RWAY. *Synapse* **2007**, *61* (2), 96-105.
(51) Shen, H.; Li, J.; Xie, X.; Yang, H.; Zhang, M.; Wang, B.; Kent, K. C.; Plutzky, J.; Guo, L. W. BRD2 regulation of sigma-2 receptor upon cholesterol deprivation. *Life Sci Alliance* **2021**, *4* (1), e201900540.
(52) Huang, Y.; Lu, H.; Zhang, L.; Wu, Z. Sigma-2 receptor ligands and their perspectives in cancer diagnosis and therapy. *Med Res Rev* **2014**, *34* (3), 532-566.
(53) McFaline-Figueroa, J. R.; Lee, E. Q. Brain Tumors. *Am J Med* **2018**, *131* (8), 874-882.
(54) Česen, M. H.; Repnik, U.; Turk, V.; Turk, B. Siramesine triggers cell death through destabilisation of mitochondria, but not lysosomes. *Cell Death Dis* **2013**, *4* (10), e818.
(55) Wang, T.; Zhang, Y.; Zhang, X.; Chen, L.; Zheng, M.; Zhang, J.; Brust, P.; Deuther-Conrad, W.; Huang, Y.; Jia, H. Synthesis and characterization of the two enantiomers of a chiral sigma-1 receptor radioligand: (*S*)-(+)- and (*R*)-(-)-[^{18}F]FBFP. *Chin Chem Lett* **2022**, *33* (7), 3543-3548.

Table of Contents Graphic